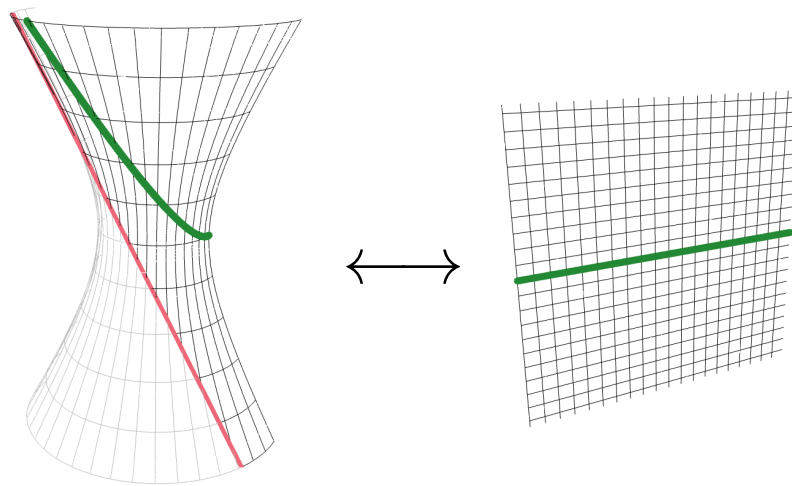


A Local Vacuum in De Sitter Space

Bart Zonneveld

Supervisors: Prof. dr. W.J.P. Beenakker and D.S. Venhoek



Department of High Energy Physics
Institute for Mathematics, Astrophysics and Particle Physics
Radboud University Nijmegen
The Netherlands

July 9, 2021

Introduction

My Master's research has been all about vacua. The concept of a vacuum has always been intriguing to me. It had something mystical to have a space with absolutely nothing in it. As a physicist, the vacuum got even more interesting: the vacuum turns out not to be 'totally empty', but rather 'as empty as possible'. Quantum Field Theory namely dictates that there will always be quantum fluctuations and therefore you might find any particle that exists in a vacuum.

This year, I learned that the concept of a vacuum has even more surprises up its sleeve. Defining a vacuum becomes tricky when we combine Quantum Field Theory with General Relativity, the theory of gravity. It turns out that our usual method to define a vacuum is not universal anymore: different observers might have different vacua and there is no good way to tell whose vacuum is 'right' and whose vacuum is 'wrong'.

The usual solution to resolve this ambiguity is to use the symmetry of the spacetime. For example in Minkowski space we can demand that the vacuum has the same symmetry as the spacetime, which gives us a unique 'right' vacuum. The mayor drawback of this method is that you need to have (enough) symmetry in the spacetime. For general spacetimes, possibly without any symmetry, we will still have the ambiguity. Furthermore, in these vacua defined by symmetry we can have inertial particle detectors that will detect a heat bath of particles, which does not match our intuition of a vacuum.

These drawbacks motivate the search for another method to resolve the ambiguity in the construction of a vacuum.

In my Master's research I investigated another proposed method to resolve the ambiguity. The method does not aim to define a vacuum that is valid for the entire spacetime. Rather, it defines a state which will be the 'right' vacuum only locally. In return, the method focuses on the behaviour of inertial particle detectors and makes sure that they behave as we would expect them to do in a vacuum. Due to its local character, we call the vacuum defined by this method 'the local vacuum'.

In my research, I focused on the question: *Can this local vacuum really exist? Or is it unphysical?* More concretely, I want to know how the local vacuum compares in terms of the expected stress energy tensor to other constructions of vacua. I focused on the de Sitter space, since it has a vacuum defined by symmetry, which we can compare with the local vacuum.

In this thesis, it will be shown that the local vacuum is currently so different from the other vacua that it is unphysical. Nonetheless, there might be a correction to the definition that will give a physical vacuum.

In this research we make some important assumptions: Firstly, in an ideal situation we should also include the quantum nature of gravity. Unfortunately, it is still unknown how to quantise gravity properly. Therefore we choose to assume that the quantum effects of gravity are small, so that they don't influence the results in this thesis. This is often called a 'semi-classical' approach.

Moreover, we even choose to only let gravity influence our particles, but don't let our particles influence the gravity. This can be seen as assuming that there is a larger source of gravity, such that the gravity caused by our particles can be neglected.

This thesis is structured as follows: in the first chapter we give some necessary background about Quantum Field Theory in curved spacetimes. In the second chapter we introduce the local vacuum and indicate how it could be constructed. In the third chapter we take a step aside and give some background information about the de Sitter space and its Bunch-Davies vacuum, which we will need to test our local vacuum definition. In chapter 4, we actually test the local vacuum by comparing it to the Bunch-Davies vacuum and to a numerical simulation. Finally, in the fifth chapter, we draw some conclusions and indicate possible new research questions.

Some of the more extensive derivations of formulas can be found in the appendices. This helps to keep the thesis readable, but still complete.

Acknowledgements

I want to thank the members of the High Energy Physics department. Unfortunately, due to the restrictions regarding the Coronavirus pandemic, it was impossible to meet physically in the department during most of the year. Thanks to an invitation to a regular informal meeting by a group of PhD-students and Post-Docs, I still felt welcome in the department, which helped me to keep going on during the pandemic.

I also want to thank Daan Janssen and Berend Visser for some discussions I had, which helped me stay critical.

Of course I want to thank my two supervisors, David and Wim. Together they helped me to learn about this nice topic and guided me through this year, while giving me a lot of freedom. We have had some good discussions about the research, which has improved this thesis. I also want to thank them for proof-reading.

Finally, I want to thank all the friends and family close to me. Although usually not so involved in my physics research, they make my life amazing.

Notation and conventions

The notations in this thesis mainly follow the conventions of [1]. In the terminology of Misner, Thorne and Wheeler [2] we use the $(- - -)$ convention. This means that our metric signature is $(+ - - -)$, that the Riemann tensor is given by

$$R^\alpha{}_{\beta\gamma\delta} = \partial_\delta \Gamma^\alpha{}_{\beta\gamma} - \partial_\gamma \Gamma^\alpha{}_{\beta\delta} + \Gamma^\alpha{}_{\delta\lambda} \Gamma^\lambda{}_{\beta\gamma} - \Gamma^\alpha{}_{\gamma\lambda} \Gamma^\lambda{}_{\beta\delta}$$

the Ricci tensor is $R_{\mu\nu} = R^\alpha{}_{\mu\alpha\nu}$ and the Einstein equations are

$$R_{\mu\nu} - \frac{1}{2}g_{\mu\nu}R = -8\pi GT_{\mu\nu}$$

Other sources, eg [3, 4], use the $(+ + +)$ convention. To change to/from this convention, change the signs of $g_{\mu\nu}$, $\square \equiv g^{\mu\nu}\nabla_\mu\nabla_\nu$, $R^\alpha{}_{\beta\gamma\delta}$, $R_{\mu\nu}$ and $T^\mu{}_\nu$, but keep $R_{\alpha\beta\gamma\delta}$, $R^\mu{}_\nu$, R and $T_{\mu\nu}$ unchanged.

The metric of the Minkowski space is denoted by $\eta_{\mu\nu} = \text{diag}(1, -1, -1, -1)$.

We use Greek indices as spacetime indices, which run from 0 to 3 and we use Latin indices as spatial indices, which run from 1 to 3.

We use the Einstein summation convention for all *Greek* indices, but we *do not* imply summation over repeated *Latin* indices.

When possible, the index 0 will refer to *conformal* time.

We take units, such that $\hbar = c = k_b = 1$.

We will use shorthand notations

$$\frac{\partial}{\partial x^\mu} f = \partial_\mu f = f_{;\mu}$$

for the partial derivative of an arbitrary object f and

$$\nabla_\mu f = f_{;\mu}$$

for the covariant derivative.

In Quantum Mechanics, we take the Heisenberg picture, where our states are spacetime independent, while our operators can have a spacetime dependency.

Contents

1	Quantum Field Theory	6
1.1	Quantum Field Theory in Minkowski space	7
1.2	Quantum Field Theory in Curved Spacetimes	11
2	The Local vacuum	20
2.1	The local vacuum	21
2.2	Example: The local vacuum in flat FRW-spaces	23
3	De Sitter Space	27
3.1	De Sitter space	27
3.2	The Bunch-Davies vacuum	29
3.3	Conformal symmetry	30
3.4	Detectors in the Bunch-Davies vacuum	33
4	Comparison Local and Bunch-Davies vacuum	35
4.1	UV-divergence	35
4.2	Cutoff regularisation	36
4.3	Dimensional regularisation	39
4.4	Interpretation	41
4.5	Simulations	44
5	Conclusion and Outlook	53
5.1	The local vacuum	53
5.2	Minimal coupling	54
5.3	Cutoff regularisation	54
	Bibliography	56
A	The Local Vacuum in Hyperbolic FRW spaces	57
B	Results for Cutoff Regularisation	60
C	Results for Dimensional Regularisation	68

Chapter 1

Quantum Field Theory

Since its development in the twentieth century, we describe elementary particles and their interactions using Quantum Field Theory. This theory states that, although the elementary particles have some particle-like behaviour, their wavelike behaviour is more fundamental.

In Quantum Field Theory we don't describe separate particles anymore. Instead, each kind of particle gets its own field which is present everywhere. Still, specific excitations of these fields can show some particle-like behaviour.

Furthermore, Quantum Field Theory resolves two issues of earlier quantum theories: in Quantum Field Theory it is no longer required that the amount of particles is conserved and the theory does not violate special relativity.

Quantum Field Theory can be applied to many different particles, using different kind of fields. In this thesis we will only focus on simple massive bosons of spin-0, which can be described by real scalar fields. This choice of spin-0 particles simplifies the computations. Extending the theory of this thesis to e.g. spin-1/2 particles could be interesting in the future.

Allowing the bosons to have mass, introduces a length-scale, which makes the theory more interesting when looking at scale-invariance, see the discussion in section 3.3.

Although Quantum Field Theory is quite successful in describing interactions between (different) particles, we do not consider these interactions in this thesis, since it introduces several extra complications.

Finally, when dealing with curved spacetimes, we neglect the back-reaction of the particles on the spacetime curvature. Instead, we impose a fixed curved spacetime, independent from the particles we describe. In this sense, we take a semi-classical approach: we will not make an attempt to quantise gravity.

In the first section, we will introduce Quantum Field Theory in flat Minkowski space. In this way, we can familiarise the reader with the conventions and we can make the differences when applying the theory in curved spacetimes more clear.

In the second section, we will look at those differences when dealing with curved spacetimes and we discuss the ambiguity and other effects that arise in this case.

The derivations in this chapter are mainly based on chapters 4, 5, 6 and 8 of [3] and sections 2.1 – 2.4, 3.2 and 3.3 of [1].

1.1 Quantum Field Theory in Minkowski space

Classical Field Theory

Before going to quantisation we will first look at the description of classical fields.

The behaviour of classical fields can be described by an action

$$S = \int dt L(t) = \int dt \int d^3x \mathcal{L}(t, \vec{x}) \quad (1.1)$$

Here $L(t)$ is called the Lagrangian and $\mathcal{L}(t, \vec{x})$ is called the Lagrangian density.

Different kind of particles are described by different Lagrangian densities. In our case, with a free real massive scalar field ϕ , the Lagrangian density is as follows:

$$\mathcal{L} = \frac{1}{2} (\eta^{\mu\nu} \partial_\mu \phi \partial_\nu \phi - m^2 \phi^2) \quad (1.2)$$

Here m is the mass of the particle that is associated with this field.

The behaviour of this field is now described by minimising the action S :

$$\begin{aligned} 0 = \delta S &= \int dt \int d^3x \left[\frac{\partial \mathcal{L}}{\partial(\partial_\mu \phi)} \partial_\mu (\delta\phi) + \frac{\partial \mathcal{L}}{\partial \phi} \delta\phi \right] \\ &= \int dt \int d^3x \left[-\partial_\mu \frac{\partial \mathcal{L}}{\partial(\partial_\mu \phi)} + \frac{\partial \mathcal{L}}{\partial \phi} \right] \delta\phi \end{aligned} \quad (1.3)$$

We assume that $\delta\phi$ vanishes at infinity, so we discarded the boundary term. Since this equation must hold for all variations $\delta\phi$, we get the Euler-Lagrange equation

$$\partial_\mu \left(\frac{\partial \mathcal{L}}{\partial(\partial_\mu \phi)} \right) - \frac{\partial \mathcal{L}}{\partial \phi} = 0 \quad (1.4)$$

For our Lagrangian density, this gives us

$$\eta^{\mu\nu} \partial_\mu \partial_\nu \phi + m^2 \phi = (\square + m^2) \phi = 0 \quad (1.5)$$

This equation is called the Klein-Gordon equation.

In Minkowski space, finding solutions of the Klein-Gordon equation is quite straightforward. We can see that we have solutions for $\phi = u_{\vec{k}}$, where $u_{\vec{k}}$ is called a mode:

$$u_{\vec{k}}(t, \vec{x}) = A_k e^{-i(\omega_k t - \vec{k} \cdot \vec{x})} \quad \text{with} \quad \omega_k = \sqrt{m^2 + k^2} \quad (1.6)$$

Here $k \equiv |\vec{k}|$ and A_k is given by normalisation.¹

¹Since the normalisation is independent of the direction, A_k can only depend on $|\vec{k}|$.

Also the complex conjugate of the mode, $u_{\vec{k}}^*$, is a solution to the Klein-Gordon equation. Since the Klein-Gordon equation is linear, any linear combination of $u_{\vec{k}}$ and $u_{\vec{k}}^*$ also yields a solution. Restricting ϕ to real values, the full solution is given by

$$\phi = \int d^3k \left(u_{\vec{k}}(t, \vec{x}) a_{\vec{k}} + u_{\vec{k}}^*(t, \vec{x}) a_{\vec{k}}^* \right) \quad (1.7)$$

Before quantisation, $a_{\vec{k}}$ and $a_{\vec{k}}^*$ are just simple coefficients.

We can define the canonical momentum field as follows:

$$\pi = \frac{\partial \mathcal{L}}{\partial(\partial_0 \phi)} = \partial_0 \phi = \int d^3k \left(\dot{u}_{\vec{k}}(t, \vec{x}) a_{\vec{k}} + \dot{u}_{\vec{k}}^*(t, \vec{x}) a_{\vec{k}}^* \right) \quad (1.8)$$

Here we have used a dot to represent a derivative with respect to time.

Quantisation

We quantise our classical field by applying a method called canonical quantisation. In this method we promote the field ϕ and the momentum field π to operators ($\hat{\phi}$ and $\hat{\pi}$) with the following equal-time commutation relations:

$$\begin{aligned} \left[\hat{\phi}(t, \vec{x}), \hat{\pi}(t, \vec{y}) \right] &= i\delta^{(3)}(\vec{x} - \vec{y}) \\ \left[\hat{\phi}(t, \vec{x}), \hat{\phi}(t, \vec{y}) \right] &= \left[\hat{\pi}(t, \vec{x}), \hat{\pi}(t, \vec{y}) \right] = 0 \end{aligned} \quad (1.9)$$

This can be achieved by promoting the coefficients $a_{\vec{k}}$ and $a_{\vec{k}}^*$ to operators $\hat{a}_{\vec{k}}$ and $\hat{a}_{\vec{k}}^\dagger$ and impose the bosonic commutation relations

$$\begin{aligned} \left[\hat{a}_{\vec{k}}, \hat{a}_{\vec{k}'}^\dagger \right] &= \delta^{(3)}(\vec{k} - \vec{k}') \\ \left[\hat{a}_{\vec{k}}, \hat{a}_{\vec{k}'} \right] &= \left[\hat{a}_{\vec{k}}^\dagger, \hat{a}_{\vec{k}'}^\dagger \right] = 0 \end{aligned} \quad (1.10)$$

This will give the following expressions for $\hat{\phi}$ and $\hat{\pi}$:

$$\hat{\phi} = \int d^3k \left(u_{\vec{k}}(t, \vec{x}) \hat{a}_{\vec{k}} + u_{\vec{k}}^*(t, \vec{x}) \hat{a}_{\vec{k}}^\dagger \right) \quad (1.11)$$

$$\hat{\pi} = \int d^3k \left(\dot{u}_{\vec{k}}(t, \vec{x}) \hat{a}_{\vec{k}} + \dot{u}_{\vec{k}}^*(t, \vec{x}) \hat{a}_{\vec{k}}^\dagger \right) \quad (1.12)$$

Checking the commutation relations (1.9) gives us

$$\begin{aligned} \left[\hat{\phi}(t, \vec{x}), \hat{\pi}(t, \vec{y}) \right] &= \int d^3k d^3k' \left(u_{\vec{k}}(t, \vec{x}) \dot{u}_{\vec{k}'}^*(t, \vec{y}) - u_{\vec{k}}^*(t, \vec{x}) \dot{u}_{\vec{k}'}(t, \vec{y}) \right) \delta^{(3)}(\vec{k} - \vec{k}') \\ &= \int d^3k |A_k|^2 (i\omega_k) \left(e^{i\vec{k} \cdot (\vec{x} - \vec{y})} + e^{-i\vec{k} \cdot (\vec{x} - \vec{y})} \right) \\ &= i \int d^3k |A_k|^2 (2\omega_k) e^{i\vec{k} \cdot (\vec{x} - \vec{y})} \end{aligned}$$

If we now cleverly choose $A_k = 1/\sqrt{2(2\pi)^3\omega_k}$, we get

$$\left[\hat{\phi}(t, \vec{x}), \hat{\pi}(t, \vec{y}) \right] = i\delta^{(3)}(\vec{x} - \vec{y}) \quad ,$$

which yields the desired result. It is easy to show that also the other commutation relations hold.

All in all we get our normalised field operator in Minkowski space

$$\hat{\phi} = \int d^3k \frac{1}{\sqrt{2(2\pi)^3\omega_k}} \left(e^{-i(\omega_k t - \vec{k} \cdot \vec{x})} \hat{a}_{\vec{k}} + e^{i(\omega_k t - \vec{k} \cdot \vec{x})} \hat{a}_{\vec{k}}^\dagger \right) \quad (1.13)$$

$$\hat{\pi} = \int d^3k (-i) \sqrt{\frac{\omega_k}{2(2\pi)^3}} \left(e^{-i(\omega_k t - \vec{k} \cdot \vec{x})} \hat{a}_{\vec{k}} - e^{i(\omega_k t - \vec{k} \cdot \vec{x})} \hat{a}_{\vec{k}}^\dagger \right) \quad (1.14)$$

How should we interpret these operators $\hat{a}_{\vec{k}}^\dagger$ and $\hat{a}_{\vec{k}}$? From standard quantum mechanics we know that these are ladder operators, which increase or decrease the energy of a state. In Quantum Field Theory these ladder operators increase or decrease the energy by creating or destroying particles. The raising operator $\hat{a}_{\vec{k}}^\dagger$ creates a particle with momentum \vec{k} and the lowering operator $\hat{a}_{\vec{k}}$ destroys such a particle.

Note that we made the choice to associate $\hat{a}_{\vec{k}}$ with the mode $u_{\vec{k}}$ and $\hat{a}_{\vec{k}}^\dagger$ with $u_{\vec{k}}^*$, while in principle we could have done it the other way around. To see why we have specifically chosen the former, we have to take a closer look at the modes.

The mode $u_{\vec{k}}^*$ describes a plane wave. The energy associated with this plane wave is given by the coefficient before the time coordinate, in this case ω_k , which is positive. This means we associate positive energy with $u_{\vec{k}}^*$ and therefore it matches the raising operator $\hat{a}_{\vec{k}}^\dagger$, which creates a particle.

On the other hand, $u_{\vec{k}}$ has negative energy ($-\omega_k$) and thus matches $\hat{a}_{\vec{k}}$, which destroys a particle.

Operators

Like in standard Quantum Mechanics, the properties of a state in Quantum Field Theory can be determined by applying operators. We construct these operators by taking the equivalent expression in classical field theory and promote ϕ and π to $\hat{\phi}$ and $\hat{\pi}$.²

For example, in classical field theory the total energy of the system at a given time is given by the Hamiltonian

$$H = \int d^3x (\pi \partial_0 \phi - \mathcal{L}) = \frac{1}{2} \int d^3x \left(\pi^2 + \sum_{i=1}^3 (\partial_i \phi)^2 + m^2 \phi^2 \right) \quad (1.15)$$

Quantising this gives the Hamiltonian operator

$$\hat{H} = \frac{1}{2} \int d^3x \left(\hat{\pi}^2 + \sum_{i=1}^3 (\partial_i \hat{\phi})^2 + m^2 \hat{\phi}^2 \right) \quad (1.16)$$

²When having multiplications of ϕ and π , this method gives some ambiguity about the ordering of the operators, since $\hat{\phi}$ and $\hat{\pi}$ do not commute. Luckily, we encounter this problem only just a few times in this thesis. In these cases we take the average over all possible orderings (Weyl ordering). This has the advantage that the resulting combination of operators is Hermitian.

Using the expressions (1.13) and (1.14) we get

$$\hat{H} = \int d^3k \frac{1}{2} \omega_k \left(\hat{a}_{\vec{k}} \hat{a}_{\vec{k}}^\dagger + \hat{a}_{\vec{k}}^\dagger \hat{a}_{\vec{k}} \right) = \int d^3k \omega_k \left(\hat{a}_{\vec{k}}^\dagger \hat{a}_{\vec{k}} + \frac{1}{2} \delta^{(3)}(0) \right) \quad (1.17)$$

From this expression we can derive

$$\hat{H} |\psi\rangle = E |\psi\rangle \Rightarrow \hat{H} \left(\hat{a}_{\vec{k}}^\dagger |\psi\rangle \right) = (E + \omega_k) \left(\hat{a}_{\vec{k}}^\dagger |\psi\rangle \right) \quad , \quad (1.18)$$

which shows again that the raising operator $\hat{a}_{\vec{k}}^\dagger$ creates a particle and adds ω_k , the energy of the particle, to the total energy.

We are now ready to define which state in Minkowski space would be the vacuum state. Quite intuitively, the vacuum is the state where it is not possible to remove any particle. In other words, the following relation for the vacuum state $|0\rangle$ holds:

$$\hat{a}_{\vec{k}} |0\rangle = 0 \quad \forall \quad \vec{k} \quad (1.19)$$

Starting with this vacuum, we can add particles using the raising operators.³ This gives

$$|n_1, n_2, \dots\rangle = \left[\prod_i \frac{\left(\hat{a}_{\vec{k}_i}^\dagger \right)^{n_i}}{\sqrt{n_i!}} \right] |0\rangle \quad (1.20)$$

This is a state with n_i particles with momentum \vec{k}_i for each i .

We can measure the amount of particles of momentum \vec{k} by applying the number operator

$$\hat{n}_{\vec{k}} = \hat{a}_{\vec{k}}^\dagger \hat{a}_{\vec{k}} \quad (1.21)$$

When applying the definition of the vacuum (1.19) to the Hamiltonian operator (1.17), one can see that the total energy in the vacuum is not zero, but is given by

$$E_0 = \int d^3k \frac{1}{2} \omega_k \delta^{(3)}(0) \quad (1.22)$$

This is clearly divergent. Partly, this is due to the fact that our universe is infinitely large. It would therefore be more useful to look at the energy *density* of the vacuum instead of the total energy. This will remove the delta-function in the expression.

But even then the expression stays divergent. As the wavenumbers k can get arbitrarily large, ω_k can also get arbitrarily large. Integrating over all ω_k therefore will give a so called UV-divergence, referring to the large wavenumbers that cause the divergence.

Eventually we need to compensate for this UV-divergence. This will be further discussed in section 4.1.

³Using proper normalisation.

1.2 Quantum Field Theory in Curved Spacetimes

Switching to curved spacetimes

Now that we have seen Quantum Field Theory in Minkowski-space, we can now extend this theory to spacetimes that are not nicely flat.

To get from Minkowski to a general spacetime, we change our Minkowski metric $\eta_{\mu\nu}$ into a general (fixed) metric $g_{\mu\nu}$, but we need more changes.

We start again with the classical action as integral of the Lagrangian density. Besides changing the metric in the action, we have to change the Minkowski spacetime element $dt d^3x$ to a more general $\sqrt{-g} d^4x$, where g is the determinant of the metric. This gives our action in a general spacetime⁴

$$S = \int \sqrt{-g} d^4x \frac{1}{2} (g^{\mu\nu} \partial_\mu \phi \partial_\nu \phi - m^2 \phi^2) \quad (1.23)$$

Using the Euler-Lagrange equation (1.4), we now get the Klein-Gordon equation for a general spacetime

$$\frac{1}{\sqrt{-g}} \partial_\mu (\sqrt{-g} g^{\mu\nu} \partial_\nu \phi) + m^2 \phi^2 = (\square + m^2) \phi = 0 \quad (1.24)$$

Note that, although the final expression looks the same as in the Minkowski case, the d'Alembert operator \square is now more complicated and dependent on the metric $g_{\mu\nu}$:

$$\square \phi = \frac{1}{\sqrt{-g}} \partial_\mu (\sqrt{-g} g^{\mu\nu} \partial_\nu \phi) = g^{\mu\nu} \nabla_\mu \nabla_\nu \phi \quad (1.25)$$

In this expression ∇_μ is the covariant derivative.

Since the Klein-Gordon equation is dependent on the chosen metric $g_{\mu\nu}$, the solutions also depend on the metric. This has as effect that we cannot give a general expression for the modes $u_{\vec{k}}$, other than noting that if $u_{\vec{k}}$ is a solution, also $u_{\vec{k}}^*$ is a solution.⁵

Still, assuming we find solutions for the specific metric we are interested in, we can do the same expansion into modes as before:⁶

$$\phi(x) = \int d^3k \left(u_{\vec{k}}(x) a_{\vec{k}} + u_{\vec{k}}^*(x) a_{\vec{k}}^* \right) \quad (1.26)$$

We can again use canonical quantisation to get our field operator

$$\hat{\phi}(x) = \int d^3k \left(u_{\vec{k}}(x) \hat{a}_{\vec{k}} + u_{\vec{k}}^*(x) \hat{a}_{\vec{k}}^\dagger \right) \quad (1.27)$$

⁴Normally, you should also change all the partial derivatives ∂_μ into covariant derivatives ∇_μ . But since our field ϕ is a scalar field, this does not change anything, until we have two covariant derivatives acting on the same field.

⁵In a general spacetime it could be that the modes cannot be identified by a vector \vec{k} , but need some other index. In some spacetimes the index will even (partly) take discrete values. In slight abuse of notation, we still will use the vector-notation \vec{k} .

⁶We are integrating over all possible values of \vec{k} . Again, if the index is not a vector, one should choose the appropriate measure, e.g. taking the sum when the index takes discrete values.

The momentum field operator is now given by

$$\hat{\pi}(x) = \sqrt{-g}g^{0\nu}\partial_\nu\hat{\phi} \quad (1.28)$$

To get the right commutation relations, the modes need to be normalised using

$$\text{Im}\left\{\int d^3k u_{\vec{k}}(t, \vec{x})\sqrt{-g}g^{0\nu}\partial_\nu u_{\vec{k}}^*(t, \vec{y})\right\} = \frac{1}{2}\delta^{(3)}(\vec{x} - \vec{y}) \quad (1.29)$$

Right now Quantum Field Theory in curved spacetimes might seem very similar to Quantum Field Theory in Minkowski-space, but there is a major difference: In Minkowski-space we could make the right connection between the raising and lowering operators on one side and the modes $u_{\vec{k}}^*$ and $u_{\vec{k}}$ on the other side. In general, this is not the case. There are many reasonable choices of $u_{\vec{k}}$ and $u_{\vec{k}}^*$.

Since the vacuum is defined by $\hat{a}_{\vec{k}}$, the choice of $u_{\vec{k}}$ determines the vacuum. When there are many different reasonable choices for $u_{\vec{k}}$, there will also be many different reasonable choices to call a vacuum. The question arises whether it is possible to choose a preferred vacuum, that all observers can agree on.

The Unruh effect

Let's first investigate whether the Quantum Field Theory in Minkowski-space is really free from this ambiguity. After all, we determined the right choice of modes by looking at their behaviour in time, but of course we could have chosen another valid time-direction.

Alice and Bob

Consider an observer (let's call her Alice) that is not moving with respect to our chosen coordinate frame. This means her trajectory can be described by

$$x_A^\mu(\tau_A) = (\tau_A, 0, 0, 0) \quad (1.30)$$

Since Alice's proper time τ_A coincides with our time-coordinate t , she will agree with our previous choice of modes. Therefore Alice's modes, which will define her vacuum, will be

$$u_{A, \vec{k}} = A_k e^{-i(\omega_k t - \vec{k} \cdot \vec{x})} \quad \text{with} \quad \omega_k = \sqrt{m^2 + k^2} \quad (1.31)$$

Now consider a second observer, Bob, moving with a constant velocity v in the x -direction with respect to our coordinate system. His trajectory will be

$$x_B^\mu(\tau_B) = \left(\frac{\tau_B}{\sqrt{1-v^2}}, \frac{v\tau_B}{\sqrt{1-v^2}}, 0, 0 \right) \quad (1.32)$$

Bob's proper time τ_B does not coincide with our time-coordinate, so Bob will not agree with Alice's choice in modes. To see what modes Bob will choose, we

do the following boost in coordinates:

$$\begin{cases} t \mapsto t' = \frac{t}{\sqrt{1-v^2}} - \frac{vx}{\sqrt{1-v^2}} \\ x \mapsto x' = -\frac{vt}{\sqrt{1-v^2}} + \frac{x}{\sqrt{1-v^2}} \\ y \mapsto y' = y \\ z \mapsto z' = z \end{cases} \quad (1.33)$$

This gives

$$x_B^{\mu'}(\tau_B) = (\tau_B, 0, 0, 0) \quad (1.34)$$

So Bob's proper time coincides with the boosted time-coordinate t' . This means that Bob will do the following choice for the modes:

$$u_{B,\vec{k}'} = A_{k'} e^{-i(\omega_{k'} t' - \vec{k}' \cdot \vec{x}')} = A_{k'} e^{-i\left(t \frac{\omega_{k'} + k'_x v}{\sqrt{1-v^2}} - x \frac{k'_x + \omega_{k'} v}{\sqrt{1-v^2}} - y k'_y - z k'_z\right)} \quad (1.35)$$

If we now make the inverse boost on k'

$$\begin{cases} k_x = \frac{k'_x + \omega_{k'} v}{\sqrt{1-v^2}} \\ k_y = k'_y \\ k_z = k'_z \end{cases} \quad (1.36)$$

$$\Rightarrow \omega_k = \frac{\omega_{k'} + k'_x v}{\sqrt{1-v^2}}, \quad (1.37)$$

we get

$$u_{B,\vec{k}'} = A_{k'} e^{-i(\omega_k t - \vec{k} \cdot \vec{x})} = \frac{A_{k'}}{A_k} u_{A,\vec{k}} \quad (1.38)$$

We see that Alice and Bob have the same modes. They only correspond to different wavenumbers (and therefore need another normalisation). This means that Alice and Bob will 'see' the same particles, only with different momentum.

This will mean that Alice and Bob will agree when there is not any particle left to be destroyed and thus they will have the same definition of the vacuum.

Bogolyubov transformations

We can express these comparisons of modes more generally using so called Bogolyubov transformations. First we note that Bob's modes $u_{B,\vec{k}'}$ and $u_{B,\vec{k}'}^*$ span all the solutions of the Klein-Gordon equation. Therefore we can express Alice's modes in terms of Bob's modes:

$$u_{A,\vec{k}} = \int d^3 k' \left(\alpha_{\vec{k}\vec{k}'} u_{B,\vec{k}'} + \beta_{\vec{k}\vec{k}'} u_{B,\vec{k}'}^* \right) \quad (1.39)$$

This gives

$$\begin{aligned} \hat{\phi} &= \int d^3 k \left(u_{A,\vec{k}} \hat{a}_{A,\vec{k}} + u_{A,\vec{k}}^* \hat{a}_{A,\vec{k}}^\dagger \right) \\ &= \int d^3 k d^3 k' \left[u_{B,\vec{k}'} \left(\alpha_{\vec{k}\vec{k}'} \hat{a}_{A,\vec{k}} + \beta_{\vec{k}\vec{k}'}^* \hat{a}_{A,\vec{k}}^\dagger \right) + u_{B,\vec{k}'}^* \left(\alpha_{\vec{k}\vec{k}'}^* \hat{a}_{A,\vec{k}}^\dagger + \beta_{\vec{k}\vec{k}'} \hat{a}_{A,\vec{k}} \right) \right] \end{aligned} \quad (1.40)$$

This gives the relation between the raising and lowering operators of two different observers:

$$\hat{a}_{B,\vec{k}'} = \int d^3k \left(\alpha_{\vec{k}\vec{k}'} \hat{a}_{A,\vec{k}} + \beta_{\vec{k}\vec{k}'}^* \hat{a}_{A,\vec{k}}^\dagger \right) \quad (1.41)$$

The coefficients $\alpha_{\vec{k}\vec{k}'}$ and $\beta_{\vec{k}\vec{k}'}$ are called Bogolyubov coefficients. They are normalised using the commutation relation (1.10), which gives

$$\begin{cases} \int d^3k \left(\alpha_{\vec{k}\vec{k}'} \alpha_{\vec{k}\vec{k}''}^* - \beta_{\vec{k}\vec{k}'}^* \beta_{\vec{k}\vec{k}''} \right) = \delta^{(3)}(\vec{k}' - \vec{k}'') \\ \int d^3k \left(\alpha_{\vec{k}\vec{k}'} \beta_{\vec{k}\vec{k}''}^* - \beta_{\vec{k}\vec{k}'}^* \alpha_{\vec{k}\vec{k}''} \right) = 0 \end{cases} \quad (1.42)$$

Let's now look how Bob will perceive Alice's vacuum (which we will denote by $|0_A\rangle$) in this general case. What happens if we apply Bob's lowering operator on Alice's vacuum?

$$\hat{a}_{B,\vec{k}'} |0_A\rangle = \int d^3k \beta_{\vec{k}\vec{k}'}^* \hat{a}_{A,\vec{k}}^\dagger |0_A\rangle \quad (1.43)$$

Bob will only agree with Alice's vacuum if this vanishes for all \vec{k}' , which is only true if $\beta_{\vec{k}\vec{k}'}$ is zero for all combinations of \vec{k} and \vec{k}' . In the last subsection we saw that in Minkowski space when Bob has a constant speed, this is true.

If we look at the expectation value of the number operator (1.21), we get

$$\langle 0_A | \hat{n}_{B,\vec{k}'} | 0_A \rangle = \langle 0_A | \hat{a}_{B,\vec{k}'}^\dagger \hat{a}_{B,\vec{k}'} | 0_A \rangle = \int d^3k |\beta_{\vec{k}\vec{k}'}|^2 \quad (1.44)$$

So $\beta_{\vec{k}\vec{k}'}$ determines the amount of particles that Bob experiences in Alice's vacuum.

Accelerating Bob

Let's see what happens when Bob gets some acceleration. To reduce the complexity of the calculations we reduce the dimension of our Minkowski-space to 2 (one timelike dimension t and one spatial dimension x) and set the mass m of our scalar particles to zero.

Alice's trajectory is still comoving with the chosen frame:

$$x_A^\mu(\tau_A) = (\tau_A, 0) \quad (1.45)$$

Again, since Alice's proper time τ_A coincides with our time-coordinate t , her modes, which will define her vacuum, will be

$$u_{A,k} = \frac{1}{\sqrt{2(2\pi)|k|}} e^{-i(|k|t - kx)} \quad (1.46)$$

Bob is taking a different trajectory:

$$x_B^\mu(\tau_B) = \left(\frac{1}{a} \sinh a\tau_B, \frac{1}{a} \cosh a\tau_B \right) \quad (1.47)$$

This trajectory is accelerating in the x -direction with acceleration a .

We see again that Bob's proper time does not coincide with our time-coordinate, so Bob will not agree with Alice's choice in modes. To see what modes Bob will choose, we do the following coordinate-transformation, only defined for $|x| > |t|$:

$$\begin{cases} t \mapsto t' = \frac{1}{a} \operatorname{artanh} \frac{t}{x} \\ x \mapsto x' = \frac{1}{2a} \ln(a^2(x^2 - t^2)) \end{cases} \quad (1.48)$$

This gives

$$x_B'^{\mu}(\tau_B) = (\tau_B, 0) \quad (1.49)$$

So Bob's proper time coincides with the time-coordinate t' .

You can check that Bob now has the following modes:⁷

$$u_{B,k'} = \frac{1}{\sqrt{2(2\pi)|k'|}} e^{-i(|k'|t' - k'x')} \quad (1.50)$$

We can now calculate the Bogolyubov coefficients, especially $\beta_{kk'}$, to check whether the vacua of Alice and Bob are corresponding.

You can show that⁸

$$\langle 0_A | \hat{n}_{B,k'} | 0_A \rangle = \int dk |\beta_{kk'}|^2 = \left[\exp\left(\frac{2\pi|k'|}{a}\right) - 1 \right]^{-1} \delta(0) \quad (1.51)$$

The divergent $\delta(0)$ can be explained by the fact that Bob will see particles in his entire space. If we look at the particle density, we only get the finite term, which is a Bose-Einstein distribution with temperature

$$T = \frac{a}{2\pi} \quad (1.52)$$

So while Alice measures a vacuum, Bob will measure a thermal bath of particles, with the temperature dependent on his acceleration. This is called the Unruh-effect after physicist Bill Unruh.

Clearly the vacua of Alice and Bob don't correspond. Does this mean that even in Minkowski space there is an ambiguity when defining a vacuum state? No, in Minkowski space the ambiguity can be resolved by using the symmetry of the spacetime. As we saw earlier, Alice's vacuum is invariant under Lorentz boosts. You can also show it is invariant under rotations and translations. In short, Alice's vacuum is invariant under all the Poincaré symmetries of Minkowski space.

On the other hand, the vacuum of the accelerated observer Bob will not be invariant under all Poincaré symmetries. Therefore we could say that Alice's vacuum is better than Bob's proposal. From now on, in Minkowski space

⁷This may be less trivial than you think. Because of the acceleration, the metric in terms of the primed coordinates is no longer constant. This means the d'Alembert operator \square is now not so trivial anymore. Only because we reduced our dimensions and chose $m = 0$, we get our usual form for our modes.

⁸For the full computation, see e.g. [3], pages 97 to 108.

we will call Alice's vacuum (and thus the vacuum of all inertial observers) *the* Minkowski vacuum.

In conclusion, the ambiguity in splitting the modes in $u_{\vec{k}}$ and $u_{\vec{k}}^*$ can be resolved in Minkowski space by using the symmetries of the spacetime. In a general spacetime, however, there will not necessarily be any symmetry. This means that in a general spacetime, it is not possible to define a single vacuum without any ambiguity.

Until now we only looked at possible vacua, which were *global*, in the sense that the state has to be a 'vacuum' everywhere in the spacetime. Maybe it is possible to circumvent the ambiguity when looking at a *local* vacuum, in the sense that the state is defined globally, but only will be a 'vacuum' at a specific region in the spacetime. In this thesis we will investigate such a local vacuum definition.

Particle Detectors

The number operator $\hat{n}_{\vec{k}}$ that Alice and Bob used in the previous subsection measures the number of particles with a specific momentum in all the space. Of course, this operator is not physical. It is impossible to have a particle detector that can scan the entire space at once.

In this subsection we will look at a more reasonable definition of a particle detector. We will follow the steps of [1], pages 48 to 54 .

We take the most simple possible detector, which will initially be in a state $|E_0\rangle$ with energy E_0 and we place it in our vacuum $|0\rangle$. We give the detector a trajectory $x^\mu(\tau)$, where τ is the proper time of the detector.

We let it interact with the field ϕ , by adding an interaction term to the Lagrangian density

$$\mathcal{L}_{\text{int.}} = c\hat{m}(\tau)\hat{\phi}(x) \quad (1.53)$$

Here $\hat{m}(\tau)$ is the monopole moment operator of the detector, which will act on the detector state and c is a coupling constant, which we assume to be small.

The monopole moment operator will excite the detector to an energy $E > E_0$. At the same time, the detector will excite the vacuum to a state $|\psi\rangle$. The amplitude for this transition is given by first order perturbation theory as

$$A = ic \langle E, \psi | \int_{-\infty}^{\infty} \hat{m}(\tau)\hat{\phi}(x(\tau)) d\tau | 0, E_0 \rangle \quad (1.54)$$

We can use the time evolution of $\hat{m}(\tau)$ in the interaction picture

$$\hat{m}(\tau) = e^{i\hat{H}_0\tau} \hat{m}(0) e^{-i\hat{H}_0\tau} \quad (1.55)$$

Here \hat{H}_0 is the unperturbed Hamiltonian operator of the detector. This gives

$$A = ic \langle E | \hat{m}(0) | E_0 \rangle \int_{-\infty}^{\infty} e^{i(E-E_0)\tau} \langle \psi | \hat{\phi}(x) | 0 \rangle d\tau \quad (1.56)$$

Now the integral in this expression is independent of the specific details of the detector. It only depends on the trajectory of the detector. On the other hand, the factor before the integral does only depend on the properties of the detector

and is independent on its trajectory and the field ϕ .

To get the probability that we excite the detector, we take the square of the modulus of this amplitude and we sum/integrate over all E and ψ . We get

$$P = c^2 \sum_E |\langle E | \hat{m}(0) | E_0 \rangle|^2 \mathcal{F}(E - E_0) \quad , \quad (1.57)$$

with

$$\mathcal{F}(E) = \int_{-\infty}^{\infty} d\tau \int_{-\infty}^{\infty} d\tau' e^{-iE(\tau-\tau')} \langle 0 | \hat{\phi}(x(\tau)) \hat{\phi}(x(\tau')) | 0 \rangle \quad (1.58)$$

This $\mathcal{F}(E)$ is called the response function. It represents the amount of available energy quanta for the detector. The monopole moment and the coupling constant c determine how much of these available quanta will actually be detected.

In Minkowski space it can be shown that, when choosing the Minkowski vacuum, the response function vanishes for all inertial trajectories.[1] This means that all inertial particle detectors will not measure any particles, as we would expect them to do.

It can also be shown that for a massless field, the response function per unit proper time⁹ for an observer with acceleration a , like Bob in the previous section, is given by [1]

$$\frac{\mathcal{F}(E)}{\Delta\tau} = \frac{E}{2\pi} \left[\exp\left(\frac{2\pi E}{a}\right) - 1 \right]^{-1} \quad (1.59)$$

We again see the Bose-Einstein distribution, with the same Unruh temperature.

Clearly, the Unruh effect does also hold for more realistic particle detectors.

Of course, one could also consider more complex detector models with a more complex interaction term than a monopole. This will give more operators $\hat{\phi}$ or even $\hat{\pi}$ in the expectation value in the expression for the response function (1.58).

We have taken the proper time intervals, e.g. in equation (1.58), from $-\infty$ to ∞ . It is possible to shorten these intervals by assuming that the detector is only switched on in the time interval that we are interested in. For this we have to assume that the detector can be switched on and off adiabatically, so that the switching itself does not influence the detector or the vacuum.

Stress Energy Tensor

Another important quantity in our vacuum is the stress energy tensor $T_{\mu\nu}$. This tensor plays an important role in one of the main equations in general relativity, the Einstein equations

$$R_{\mu\nu} - \frac{1}{2}g_{\mu\nu}R = -8\pi GT_{\mu\nu} \quad (1.60)$$

⁹The response function per unit time is found by taking only one of the proper time integrals in equation (1.58).

Here G is the gravitational constant. The stress energy tensor on the right hand side acts as a source for the curvature on the left side.

Although we work in the semi-classical approach, where we neglect the back-reaction of our fields on the spacetime curvature and therefore totally ignore equation (1.60), it is still important¹⁰ to compute the stress energy tensor. Firstly, it can show us whether our semi-classical approach is a reasonable approximation and, secondly, it could be valuable information when you go to the next level and start quantising gravity.

The Einstein equations can be derived by adding a gravitational part to our action:

$$S^{\text{grav}} = \frac{1}{16\pi G} \int \sqrt{-g} d^4x R \quad (1.61)$$

When we vary this with respect to the metric, we get

$$\frac{\delta S^{\text{grav}}}{\delta g^{\mu\nu}} = \frac{\sqrt{-g}}{16\pi G} \left(R_{\mu\nu} - \frac{1}{2} g_{\mu\nu} R \right) \quad (1.62)$$

Since the total action should be minimised, this has to be compensated by the variation of our original action, which we will call S^{m} :

$$\begin{aligned} \frac{\delta S^{\text{grav}}}{\delta g^{\mu\nu}} + \frac{\delta S^{\text{m}}}{\delta g^{\mu\nu}} &= 0 \\ \Rightarrow R_{\mu\nu} - \frac{1}{2} g_{\mu\nu} R &= -8\pi G \left(\frac{2}{\sqrt{-g}} \frac{\delta S^{\text{m}}}{\delta g^{\mu\nu}} \right) \end{aligned}$$

This gives us the expression for the stress energy tensor:

$$T_{\mu\nu} = \frac{2}{\sqrt{-g}} \frac{\delta S^{\text{m}}}{\delta g^{\mu\nu}} \quad (1.63)$$

For the action for the free real massive scalar field in curved spacetimes, (1.23), this gives

$$T_{\mu\nu} = \partial_\mu \phi \partial_\nu \phi - \frac{1}{2} g_{\mu\nu} g^{\alpha\beta} \partial_\alpha \phi \partial_\beta \phi + \frac{1}{2} g_{\mu\nu} m^2 \phi^2 \quad (1.64)$$

We can make this an operator by using canonical quantisation:

$$\hat{T}_{\mu\nu}(x) = \partial_\mu \hat{\phi}(x) \partial_\nu \hat{\phi}(x) - \frac{1}{2} g_{\mu\nu}(x) g^{\alpha\beta}(x) \partial_\alpha \hat{\phi}(x) \partial_\beta \hat{\phi}(x) + \frac{1}{2} g_{\mu\nu}(x) m^2 \hat{\phi}(x)^2 \quad (1.65)$$

In this equation we made the spacetime-dependence more explicit.

¹⁰Arguably even more important.

Summary

Elementary particles can be described using Quantum Field Theory by excitations in a specific field. Different particles have different fields. In this thesis we focus on a free real massive scalar field to keep calculations simple, but still interesting.

The behaviour of this field can be described by the Lagrangian density. The Euler-Lagrange equation gives us the Klein-Gordon equation, which we can solve in Minkowski space. This gives us an expansion of our field in modes.

To change our field into a quantum field, we use canonical quantisation. This promotes our field ϕ and momentum field π into field operators. The coefficients in our mode expansion are promoted to raising and lowering operators that we can interpret to create and destroy particles. By associating an energy to our modes, we can make sure we match the right raising or lowering operator with each mode. We can also define the vacuum as the state where applying each lowering operator gives zero.

When we move from a flat spacetime to a fixed curved spacetime, we need slight modifications to the Lagrangian density to adapt it to the new metric. We get a similar looking Klein-Gordon equation, but the operator involved is now dependent on the metric. It is also impossible to get a general expression for our modes.

Furthermore, in a curved spacetime there is no good way anymore to match the raising and lowering operator with the right modes. Different choices can be made, which may give different vacuum states.

In Minkowski space the vacuum state coincides for all inertial observers. Accelerated observers will not agree on the vacuum of the inertial observers. Instead, they will measure a heat bath of particles, dependent on their acceleration. This is called the Unruh effect.

Demanding that the vacuum is invariant under all symmetries of Minkowski spacetimes, only leaves the vacuum of the initial observers and therefore lifts the ambiguity. We will call this state *the* Minkowski vacuum. This trick only works when we have enough symmetry, so in spacetimes without symmetry, it is not possible to lift the ambiguity globally.

We can construct a more realistic model of a particle detector, which works locally. Also in this model the Unruh effect is present.

The stress energy tensor can also be quantised. Although we ignore the back-reaction of this tensor in our semi-classical approach, it is an important quantity for checking how reasonable our approach is and it can be valuable information when constructing a full quantum theory of gravity.

Chapter 2

The Local vacuum

In the last chapter we showed that there is an ambiguity when doing canonical quantisation in Quantum Field Theory. We have to split the solutions to the Klein-Gordon equation into two parts: one part, u_k^* , we associate with \hat{a}_k^\dagger and thus with creating a particle and one part, $u_{\bar{k}}$, we associate with $\hat{a}_{\bar{k}}$ and thus with destroying a particle. Unfortunately, it depends on the observer which splitting is sensible. Only when there is enough symmetry, for example in Minkowski space, we can use the symmetry to choose the best splitting and get rid of the ambiguity.

So in a general spacetime, possibly without any symmetry, we cannot choose one unambiguous vacuum state for our entire universe. But maybe we can do the next best thing and construct a vacuum state that is unambiguously defined locally, somewhere in our universe: a vacuum state that all *local* inertial observers can agree on.

In the last chapter we also showed that we can construct a realistic model of a particle detector (at least more realistic than the number operator), using the local operator $\hat{\phi}(x)$. Having a local definition of a vacuum also matches this switch from a global number operator to a local, more realistic particle detector.

In the first section we will define our local vacuum and show how it can be constructed. In the second section we will explicitly calculate the splitting of modes for the local vacuum in (spatially) flat Friedmann-Robertson-Walker space (FRW-space).¹ Another example of the construction of the local vacuum, using (spatially) hyperbolic FRW-space, is given in appendix A.²

The concept of the local vacuum, as introduced in this chapter, is an idea by David Venhoeck. The definition of the local vacuum is mainly based on his work, which, at this moment, is yet to be published.

¹Also known as Friedmann space, Robertson-Walker (RW) space, Friedmann-Lemaître (FL) space or Friedmann-Lemaître-Robertson-Walker (FLRW) space.

²This second example is not needed for this thesis, but could be useful in the future.

2.1 The local vacuum

When constructing this new definition of the vacuum, which we will call ‘the local vacuum’, we focus on the experience of local, inertial observers. This will also match how we would do measurements in reality. These observers can observe the state of our quantum field using a particle detector that works locally: it does only depend on the field operator at the trajectory of the detector, not anywhere else in the universe.

Specifically, we are interested in the response function $\mathcal{F}(E)$ (see equation (1.58)), which we can see as the available energy quanta for the detector, which, for a simple monopole detector, is given by

$$\mathcal{F}(E) = \int_{-\infty}^{\infty} d\tau \int_{-\infty}^{\infty} d\tau' e^{-iE(\tau-\tau')} \langle 0 | \hat{\phi}(x(\tau)) \hat{\phi}(x(\tau')) | 0 \rangle \quad (2.1)$$

If we assume that the detector can be switched on and off adiabatically, we can reduce the proper time intervals that we integrate over. Ultimately, with slight disregard for the quantum nature of the detector, we can see that the available energy quanta *at a certain moment* τ_0 is determined by

$$\langle 0 | \hat{\phi}(x(\tau_0)) \hat{\phi}(x(\tau_0)) | 0 \rangle \quad (2.2)$$

We can therefore heuristically say that an observer only experiences a vacuum at a spacetime point x_0 , when

$$\langle 0 | \hat{\phi}(x_0) \hat{\phi}(x_0) | 0 \rangle \quad (2.3)$$

behaves *as one could expect for a vacuum*.

Of course there is only one non-disputed vacuum that we can use to see what this ‘right behaviour’ of expression (2.3) is: the Minkowski vacuum.

So we can say that a state $|0\rangle$ behaves as a vacuum at spacetime point x_0 when

$$\langle 0 | \hat{\phi}(x_0) \hat{\phi}(x_0) | 0 \rangle = \langle 0_M | \hat{\phi}_M \hat{\phi}_M | 0_M \rangle \quad (2.4)$$

with $|0_M\rangle$ being the Minkowski vacuum and $\hat{\phi}_M$ the field operator in Minkowski space.

Of course we also want this vacuum-like behaviour when we take more complicated detectors than this simple monopole. This means that we can change the expression (2.3) to an expression with more operators $\hat{\phi}(x_0)$ or even operators $\hat{\pi}(x_0)$.

This makes that our state $|0\rangle$ behaves as a vacuum at time and position x_0 using all possible local detectors, when

$$\langle 0 | O(\hat{\phi}(x_0), \hat{\pi}(x_0)) | 0 \rangle = \langle 0_M | O(\hat{\phi}_M, \hat{\pi}_M) | 0_M \rangle \quad (2.5)$$

for any polynomial of two operators $O(\hat{A}, \hat{B})$.

We are now ready to introduce our definition of the local vacuum, where we extend this vacuum-like behaviour to a larger spacetime region \mathcal{S} :

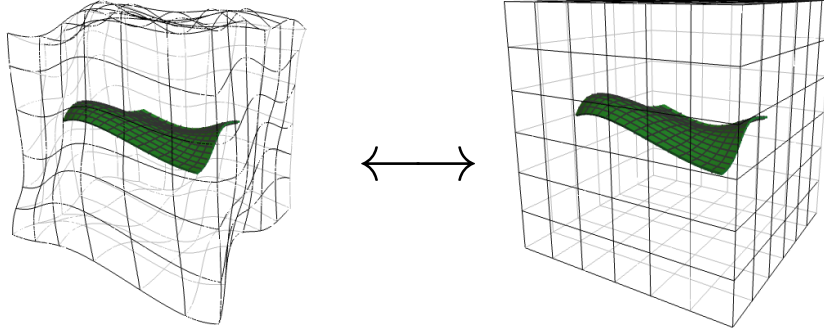


Figure 2.1: The concept of the local vacuum: on the left side we have our curved spacetime, with in green the spacetime region \mathcal{S} , for which we define the local vacuum. The spacetime region is embedded in Minkowski space on the right side, using an isometric map. The local vacuum is now defined such that it acts the same on local detectors in the spacetime region \mathcal{S} as the Minkowski vacuum acts on those detectors in the embedded region.

Definition local vacuum: A system with a real scalar massive quantum field $\hat{\phi}$ is in a local vacuum state $|0_L\rangle$ for a defining spacetime region \mathcal{S} , when for every $x \in \mathcal{S}$ and every polynomial of two operators $O(\hat{A}, \hat{B})$ the following relation holds:

$$\langle 0_L | O(\hat{\phi}(x), \hat{\pi}(x)) | 0_L \rangle = \langle 0_M | O(\hat{\phi}_M(y), \hat{\pi}_M(y)) | 0_M \rangle \quad (2.6)$$

Here $|0_M\rangle$ is the Minkowski vacuum and $\hat{\phi}_M(y)$ the field operator in Minkowski space at spacetime point y . This point y should be given by a map $x \mapsto y(x)$, which is isometric for all $x \in \mathcal{S}$. This means that the metric elements in the curved spacetime, restricted to the region \mathcal{S} , equal the metric elements in Minkowski space, restricted to the projection of that region, using x and y as coordinates respectively.

Note that not for all spacetime regions \mathcal{S} we can define a corresponding local vacuum. In fact, since there should be an isometry between the region \mathcal{S} and Minkowski space, it should be possible to embed the region in Minkowski space. In general, this will mean that the region needs to have at least one dimension less than our spacetime.³

How local is the local vacuum?

Let's have a closer look at the name 'local vacuum' and indicate what we exactly mean with 'local'.

It is *not* true that the local vacuum is only defined in this local spacetime region. In fact the state is defined in the whole universe. As we are working

³Only in trivial cases, where (a part of) our spacetime is flat, we can embed a spacetime region in Minkowski space without reducing the dimension.

in the Heisenberg picture, the state is independent of the position in the spacetime, so if it is defined in the local spacetime region, it automatically is defined everywhere.

So what makes our local vacuum local? And why is the defining spacetime region \mathcal{S} important?

In fact, outside \mathcal{S} , the local vacuum is not a special state. In general, it will not have the property (2.6) and thus will be a state as any other state. Only inside \mathcal{S} the local vacuum will have its special property (2.6), which makes it behave like a vacuum for local, inertial observers.

If we have another spacetime region where we have a local vacuum, that state will in general be different from our previous local vacuum. That is the local character of this local vacuum.

2.2 Example: The local vacuum in flat FRW-spaces

We will now construct the local vacuum in so called (spatially) flat FRW-spaces.⁴ This will be an important example and will be used in the remainder of this thesis.

Friedmann-Robertson-Walker space

The flat Friedmann-Robertson-Walker space (FRW-space) is a homogeneous, isotropic spacetime. It is defined by the flat FRW-metric

$$ds^2 = dt^2 - a^2(t) \left[\sum_i (dx^i)^2 \right] \quad (2.7)$$

The factor $a(t)$ is called the scale factor. The scale factor determines the evolution of the universe. When it is increasing in time, the universe is expanding, when it decreases, the universe is contracting.

We can rescale our time t using the scale factor:

$$d\eta = \frac{dt}{a(t)} \quad (2.8)$$

This gives us the following expression for the metric:

$$ds^2 = a^2(\eta) \left[d\eta^2 - \sum_i (dx^i)^2 \right] \quad (2.9)$$

This new time-coordinate η is called ‘conformal time’. Using conformal time has its advantages when considering conformal transformations (we will discuss them in section 3.3). Therefore we will use conformal time in this thesis.⁵

⁴It is called ‘flat’ because the spatial slices of the metric have no curvature. Nonetheless, the curvature can be non-zero when also considering time.

⁵The index 0 will from now on refer to the conformal time, unless specified otherwise.

The non-zero Christoffel symbols are:

$$\Gamma_{00}^0 = \Gamma_{ii}^0 = \Gamma_{0i}^i = \Gamma_{i0}^i = \frac{\dot{a}}{a} \quad (2.10)$$

where a dot represents differentiation with respect to conformal time.

This gives the following Riemann tensor components:

$$R^0_{i0i} = -\frac{\ddot{a}a - \dot{a}^2}{a^2} \quad , \quad R^i_{jij} = -\frac{\dot{a}^2}{a^2} \quad (i \neq j) \quad (2.11)$$

All other components are either related by symmetry or zero.

This gives the following non-zero components of the Ricci tensor:

$$R_{00} = 3\frac{\ddot{a}a - \dot{a}^2}{a^2} \quad , \quad R_{ii} = -\frac{\ddot{a}a + \dot{a}^2}{a^2} \quad (2.12)$$

and the Ricci scalar

$$R = 6\frac{\ddot{a}}{a^3} \quad (2.13)$$

Creating the isometric map

To construct our local vacuum, we need to identify a defining spacetime region where our local vacuum will have its special meaning. Except for the trivial case that the scale factor is constant, we have to reduce the dimension of this spacetime region to make the isometric map to Minkowski space.

We will take the simplest choice by taking a spatial slice at conformal time $\eta = \eta_0$ as our defining spacetime region. This slice is very easy to embed in Minkowski space.

On the slice we have the induced metric

$$ds_3^2 = -a_0^2 \sum_i (dx^i)^2 \quad (2.14)$$

where we introduce the short-hand notation $a_0 = a(\eta_0)$, which is a constant.

We can now embed this spatial slice in Minkowski space by the following map:

$$x^i \mapsto (t_M, x_M^i) = (0, a_0 y^i) \quad (2.15)$$

where t_M and x_M^i are our usual Minkowski coordinates.

Our slice is thus mapped to a spatial slice in Minkowski space at $t_M = 0$ and with scaled coordinates.

The induced metric is

$$ds_3^2 = -\sum_i (dx_M^i)^2 = -a_0^2 \sum_i (dy^i)^2 \quad (2.16)$$

which is the same as our original slice, thus the map is isometric.

Let's see what the influence of the scaled spatial coordinates is on our Minkowski modes.

The full Minkowski metric with the scaled spatial coordinates is

$$ds^2 = dt_M^2 - a_0^2 \left[\sum_i (dy^i)^2 \right] \quad (2.17)$$

Using this we can find the solutions of the Klein-Gordon equation (1.24)

$$u_{M,\vec{k}}(t_M, y^i) = A_k e^{-i(\omega_k t_M - \vec{k} \cdot \vec{y})} \quad \text{with} \quad \omega_k = \sqrt{m^2 + k^2/a_0^2} \quad (2.18)$$

Normalising using equation (1.29) gives

$$u_{M,\vec{k}}(t_M, y^i) = \frac{1}{\sqrt{2(2\pi a_0)^3 \omega_k}} e^{-i(\omega_k t_M - \vec{k} \cdot \vec{y})} \quad (2.19)$$

Furthermore we get the following expression for the derivative with respect to Minkowski time:

$$\frac{\partial}{\partial t_M} u_{M,\vec{k}}(t_M, y^i) = -i \sqrt{\frac{\omega_k}{2(2\pi a_0)^3}} e^{-i(\omega_k t_M - \vec{k} \cdot \vec{y})} \quad (2.20)$$

Making the match

To fulfill the expression (2.6) in the definition of the local vacuum, we first have to make sure that $\hat{\phi}(\eta_0, x^i)$ acts on the vacuum like $\hat{\phi}_M(0, y^i)$ acts on the Minkowski vacuum. This can be achieved by taking

$$\begin{aligned} u_{\vec{k}}(\eta_0, x^i) &= u_{M,\vec{k}}(0, x^i) \\ &= \frac{1}{\sqrt{2(2\pi a_0)^3 \omega_k}} e^{i\vec{k} \cdot \vec{x}} \quad \text{with} \quad \omega_k = \sqrt{m^2 + k^2/a_0^2} \end{aligned} \quad (2.21)$$

Similarly, to match the behaviour of $\hat{\pi}(\eta_0, x^i)$ and $\hat{\pi}_M(0, y^i)$, we take⁶

$$\begin{aligned} a_0^2 \dot{u}_{\vec{k}}(\eta_0, x^i) &= a_0^3 \frac{\partial}{\partial t_M} u_{M,\vec{k}}(0, x^i) \\ \Rightarrow \dot{u}_{\vec{k}}(\eta_0, x^i) &= -i \sqrt{\frac{\omega_k}{2(2\pi)^3 a_0}} e^{i\vec{k} \cdot \vec{x}} \end{aligned} \quad (2.22)$$

These two matching conditions give us the initial conditions of the modes at our spatial slice. We can get the modes for the entire spacetime by solving the Klein-Gordon equation for the curved spacetime (1.24) using these initial conditions. The explicit solution will depend on the chosen scale factor, so we don't have a general expression.⁷

As we have seen in the last chapter, the choice of mode splitting, this time made by the boundary conditions above, is automatically a choice of a vacuum. So we have now constructed our local vacuum.

⁶Note the different power of a_0 due to the different $\sqrt{-g}$ in both spaces.

⁷In this thesis we are mostly interested in the behaviour of the local vacuum on the spatial slice. Just having the initial conditions is sufficient for this.

Summary

We define a state, called the local vacuum, which is aimed at giving the same experience to inertial observers in a certain region as they would experience in the Minkowski vacuum.

Based on the response function for various local particle detectors, we define that the local vacuum has the same expectation values for combinations of field operators inside a certain defining region as the expectation value in Minkowski space.

In practice we take some part of our spacetime, generally with reduced dimension, and embed this region in Minkowski space.

Contrary to what the name might suggest, the local vacuum for a certain region is defined in the entire spacetime. Nonetheless, outside its defining region the state has no special properties. Only inside its region it matches the Minkowski vacuum. This is why it is called the local vacuum.

We can construct a local vacuum in flat FRW-space. Since spatial slices of FRW-space are flat, they are quite straightforward to embed in Minkowski space. Therefore we chose an arbitrary spatial slice of FRW-space as the defining region of the local vacuum.

Requiring that a detector experiences a Minkowski vacuum on this spatial slice, we get the modes and their derivatives with respect to conformal time on the slice. These initial conditions can be used together with the Klein-Gordon equation to give the full modes. Once we have the full modes, they automatically define our local vacuum as we saw in chapter 1.

Chapter 3

De Sitter Space

Before we can apply the definition of the local vacuum to arbitrary spacetimes, we first want to check whether this state is physical. To test this we have to compare it with some other vacuum definition.

Of course we cannot test the local vacuum in Minkowski space, since, by construction, it will be equal to the Minkowski vacuum. So we need a more complex spacetime. On the other hand, we need a reasonable other definition for a vacuum to compare it with. For spacetimes which are too complex, we don't have such definitions.

This brings us to the de Sitter space: it has curvature, which makes the local vacuum non-trivial, but it has also enough symmetry to have an alternative vacuum definition: the Bunch-Davies vacuum.

In the first section we introduce the de Sitter space and its most important properties. In the second section we introduce the Bunch-Davies vacuum. In the third section we discuss the concept of conformal symmetry and how this relates to the de Sitter space. In the last section we look at the behaviour of particle detectors in the Bunch-Davies vacuum.

3.1 De Sitter space

To define de Sitter space, we start with five-dimensional Minkowski space, with coordinates (u', w', x', y', z') and corresponding metric

$$ds_5^2 = (du')^2 - (dw')^2 - (dx')^2 - (dy')^2 - (dz')^2 \quad (3.1)$$

Now the de Sitter space is a hyperboloid embedded in this space given by

$$-(u')^2 + (w')^2 + (x')^2 + (y')^2 + (z')^2 = \alpha^2 \quad (3.2)$$

with α being a constant.[4] As we will see later, α determines the curvature of the de Sitter space.

We can choose the coordinates (t', χ, θ, ϕ) on the hyperboloid as follows:

$$\begin{cases} u' = \alpha \sinh(t'/\alpha) \\ w' = \alpha \cosh(t'/\alpha) \cos \chi \\ x' = \alpha \cosh(t'/\alpha) \sin \chi \cos \theta \\ y' = \alpha \cosh(t'/\alpha) \sin \chi \sin \theta \cos \phi \\ z' = \alpha \cosh(t'/\alpha) \sin \chi \sin \theta \sin \phi \end{cases} \quad (3.3)$$

This induces the following metric in de Sitter space, which is valid everywhere:

$$ds^2 = (dt')^2 - \alpha^2 \cosh^2(t'/\alpha) [d\chi^2 + \sin^2 \chi (d\theta^2 + \sin^2 \theta d\phi^2)] \quad (3.4)$$

If we only consider the region $u' + w' > 0$, we can choose a more convenient set of coordinates (t, x, y, z) :

$$\begin{cases} u' = \alpha \sinh(t/\alpha) + \frac{e^{t/\alpha}}{2\alpha} (x^2 + y^2 + z^2) \\ w' = \alpha \cosh(t/\alpha) - \frac{e^{t/\alpha}}{2\alpha} (x^2 + y^2 + z^2) \\ x' = x e^{t/\alpha} \\ y' = y e^{t/\alpha} \\ z' = z e^{t/\alpha} \end{cases} \quad (3.5)$$

This induces the metric

$$ds^2 = dt^2 - e^{2t/\alpha} [dx^2 + dy^2 + dz^2] \quad (3.6)$$

We can recognise the shape of the flat FRW-metric that we saw in section 2.2. We can switch to conformal time

$$\eta = -\alpha e^{-t/\alpha} \quad (3.7)$$

Note that it runs from $-\infty$ to 0. This gives metric

$$ds^2 = \frac{\alpha^2}{\eta^2} [d\eta^2 - dx^2 - dy^2 - dz^2] \quad (3.8)$$

So the scale factor is given by $a(\eta) = -\alpha/\eta$. Note that η is always negative, so we need a minus sign to keep the scale factor positive.

We can now use equation (2.11) to show that the Riemann tensor has components

$$R^0_{i0i} = R^i_{jij} = -\frac{1}{\eta^2} \quad (i \neq j) \quad (3.9)$$

All other components are either related by symmetry or zero. We can cast this into another shape:

$$R_{\alpha\beta\gamma\delta} = \frac{1}{\alpha^2} (g_{\alpha\gamma} g_{\beta\delta} - g_{\alpha\delta} g_{\beta\gamma}) \quad (3.10)$$

The fact that the Riemann tensor can be written only in terms of the metric, shows us that the de Sitter space is homogeneous and isotropic: There is no preferred point, nor preferred direction. This makes de Sitter space a maximally symmetric space. [4]

We can calculate the Ricci scalar

$$R = \frac{12}{\alpha^2} \quad (3.11)$$

This is a constant (as it should be, since the space is homogeneous). We can also see now that the curvature of de Sitter space is determined by α .

The fact that de Sitter space is maximally symmetric tells us that it has 10 symmetries: We have the 3 spatial translations and 3 spatial rotations, as we know from Minkowski space. We also will have 3 ‘boosts’ and 1 ‘translation in time’, but these will be different than in the Minkowski case.

Finally, we want to mention briefly that we can also choose a third set of coordinates $(\bar{t}, \bar{\chi}, \bar{\theta}, \bar{\phi})$ for the region $w' \geq \alpha$ defined by

$$\begin{cases} u' = \alpha \sinh(\bar{t}/\alpha) \cosh \bar{\chi} \\ w' = \alpha \cosh(\bar{t}/\alpha) \\ x' = \alpha \sinh(\bar{t}/\alpha) \sinh \bar{\chi} \cos \bar{\theta} \\ y' = \alpha \sinh(\bar{t}/\alpha) \sinh \bar{\chi} \sin \bar{\theta} \cos \bar{\phi} \\ z' = \alpha \sinh(\bar{t}/\alpha) \sinh \bar{\chi} \sin \bar{\theta} \sin \bar{\phi} \end{cases} \quad (3.12)$$

This induces the metric:

$$ds^2 = d\bar{t}^2 - \alpha^2 \sinh^2(\bar{t}/\alpha) \left[d\bar{\chi}^2 + \sinh^2 \bar{\chi} \left(d\bar{\theta}^2 + \sin^2 \bar{\theta} d\bar{\phi}^2 \right) \right] \quad (3.13)$$

This is a spatial *hyperbolic* FRW-metric. We will not use these coordinates in this thesis, but together with the construction of the local vacuum for spatial hyperbolic FRW-spaces in appendix A, it might be interesting to see whether investigating the local vacuum in this case yields the same results as in this thesis.

3.2 The Bunch-Davies vacuum

In chapter 1 we saw that we can define a vacuum by solving the Klein-Gordon equation and then resolve the ambiguity when splitting these solutions into modes $u_{\vec{k}}$ and $u_{\vec{k}}^*$. Since de Sitter space is maximally symmetric, we can split the modes using the symmetry.

Let’s first solve the Klein-Gordon equation (1.24)

$$0 = (\square + m^2)\phi = \frac{\eta^2}{\alpha^2} \left(\partial_0 \partial_0 - \frac{2}{\eta} \partial_0 - \sum_i \partial_i \partial_i + \frac{m^2 \alpha^2}{\eta^2} \right) \phi \quad (3.14)$$

We take as ansatz for our modes

$$u_{\vec{k}} = v_k(\eta) e^{i\vec{k} \cdot \vec{x}} \quad (3.15)$$

Note that our temporal part v_k only depends on the modulus of the wavenumber $k = |\vec{k}|$, since we want our modes to have no preferred direction.

The ansatz yields

$$\ddot{v}_k - \frac{2}{\eta} \dot{v}_k + \left(k^2 + \frac{m^2 \alpha^2}{\eta^2} \right) v_k = 0 \quad (3.16)$$

We can take $z = -k\eta$ and recast the equation to

$$z^2 \frac{\partial^2}{\partial z^2} \left(\frac{v_k}{z^{3/2}} \right) + z \frac{\partial}{\partial z} \left(\frac{v_k}{z^{3/2}} \right) + \left[z^2 - \left(\frac{9}{4} - m^2 \alpha^2 \right) \right] \left(\frac{v_k}{z^{3/2}} \right) = 0 \quad (3.17)$$

This is the form of Bessel's differential equation, which has Bessel functions as solutions:

$$v_k(\eta) = (-k\eta)^{3/2} [A_k J_\nu(-k\eta) + B_k Y_\nu(-k\eta)] \quad \text{with} \quad \nu^2 = \frac{9}{4} - m^2 \alpha^2 \quad (3.18)$$

Here J_ν and Y_ν are Bessel functions of the first and second kind respectively. For simplicity, we assume $m\alpha < 3/2$, so ν is real.

We now only need to determine the ratio between A_k and B_k to fix our modes (the rest is fixed by normalisation).

For example in [1] and [3], it is shown that the desired choice is $B_k = iA_k$. Normalisation using equation (1.29) gives us¹

$$u_{\vec{k}} = v_k(\eta) e^{i\vec{k} \cdot \vec{x}} = \frac{1}{\pi \alpha} \sqrt{\frac{(-\eta)^3}{32}} H_\nu^{(1)}(-k\eta) e^{i\vec{k} \cdot \vec{x}} \quad (3.19)$$

Here $H_\nu^{(1)}(z) \equiv J_\nu(z) + iY_\nu(z)$ is called the Hankel function of the first kind. For real ν and z , its complex conjugate is $H_\nu^{(2)}(z) \equiv J_\nu(z) - iY_\nu(z)$, which is called the Hankel function of the second kind.

The vacuum that is now defined by this choice of modes is called the Bunch-Davies vacuum.

3.3 Conformal symmetry

The form of the metric of the de Sitter space using conformal time is quite special: it is the Minkowski metric with an overall scale factor. We can even interpret de Sitter space as Minkowski space that we transformed by applying a spacetime dependent scaling. This type of transformation is called a conformal transformation. The general form is

$$g_{\mu\nu}(x) \mapsto \bar{g}_{\mu\nu}(x) = \Omega^2(x) g_{\mu\nu}(x) \quad (3.20)$$

Here $\Omega(x)$ is a continuous, non-vanishing, finite real function.

A very interesting case would be if our physics would be invariant under these conformal transformations.

¹Note that the references use a different convention for which mode is $u_{\vec{k}}$ and which $u_{\vec{k}}^*$, so they get a Hankel function of the *second* kind.

Firstly, note that these conformal transformations include the simple rescaling of coordinates. If the physics is invariant, it would mean that the theory would be scale-invariant. This has as a consequence that the mass of our particles should be zero. Any finite mass would introduce a length-scale, which breaks the scale-invariance.

Secondly, more modifications are needed. Let's have a look at the action with $m = 0$, as we derived in equation (1.23), but now generalised to d dimensions:²

$$S = \int \sqrt{-g} d^d x \frac{1}{2} g^{\mu\nu} \partial_\mu \phi \partial_\nu \phi \quad (3.21)$$

As S has no length-dimension we can see that our field ϕ has a length-dimension of $1 - d/2$. This means that with a conformal transformation we have to scale it accordingly:

$$\phi \mapsto \bar{\phi} = \Omega^{1-d/2} \phi \quad (3.22)$$

We can now focus on the Klein-Gordon equation in the massless case:

$$\square \phi = 0 \quad (3.23)$$

A conformal transformation gives:

$$\begin{aligned} 0 = \bar{\square} \bar{\phi} &= \frac{1}{\sqrt{-\Omega^{2d}g}} \partial_\mu \left[\sqrt{-\Omega^{2d}g} \Omega^{-2} g^{\mu\nu} \partial_\nu \left(\Omega^{1-d/2} \phi \right) \right] \\ &= \Omega^{-1-d/2} \left[\square - \frac{(d-2)(d-4)}{4} \Omega^{-2} g^{\mu\nu} \partial_\mu \Omega \partial_\nu \Omega - \frac{d-2}{2} \Omega^{-1} \square \Omega \right] \phi \end{aligned} \quad (3.24)$$

We can clearly see that our physics is not invariant under conformal transformations. Fortunately, it is not hard to fix it. It can be shown that the Ricci scalar has the following conformal transformation: [1]

$$R \mapsto \bar{R} = \Omega^{-2} \left[R + (d-1)(d-4) \Omega^{-2} g^{\mu\nu} \partial_\mu \Omega \partial_\nu \Omega + 2(d-1) \Omega^{-1} \square \Omega \right] \quad (3.25)$$

We can easily see that when we take

$$\left(\square + \frac{d-2}{4(d-1)} R \right) \phi = 0 \quad (3.26)$$

this expression is invariant under conformal transformations.

To get this Klein-Gordon equation we have to add an extra term to our action:

$$S = \int \sqrt{-g} d^d x \frac{1}{2} (g^{\mu\nu} \partial_\mu \phi \partial_\nu \phi - \xi R \phi^2) \quad (3.27)$$

Where taking $\xi = (d-2)/(4(d-1))$ (or in 4 dimensions $\xi = 1/6$)³ is called the conformal coupling and gives invariant physics under conformal transformations. To get our old action we take $\xi = 0$, which is called minimal coupling.

The coupling ξ gives a measure of how much our matter is coupled to gravity. In the minimal coupling it is only coupled by the metric itself, for non-zero ξ we also have a coupling to the Ricci scalar.

²We need expressions in d dimensions for our dimensional regularisation later in this thesis. The results of previous sections can be generalised to d dimensions in a quite straightforward manner, but for conformal transformations, this is more tricky, so we will do it in d dimensions directly.

³For this coupling it is not straightforward to generalise to d dimensions. That is why we did this section in d dimensions. We can now go back to 4 dimensions.

Changes in the action

Although for the massive fields that we investigate in this thesis, the mass breaks the conformal symmetry, we can still add this extra term to the action.⁴

This gives us a few modifications: to our action (1.23)

$$S = \int \sqrt{-g} d^4x \frac{1}{2} (g^{\mu\nu} \partial_\mu \phi \partial_\nu \phi - (m^2 + \xi R) \phi^2) \quad (3.28)$$

to the Klein-Gordon equation (1.24)

$$(\square + m^2 + \xi R) \phi = 0 \quad (3.29)$$

and the stress energy tensor (1.64) (in d dimensions) [1]

$$\begin{aligned} T_{\mu\nu} = & (1 - 2\xi) \phi_{;\mu} \phi_{;\nu} + \left(2\xi - \frac{1}{2}\right) g_{\mu\nu} g^{\alpha\beta} \phi_{;\alpha} \phi_{;\beta} - 2\xi \phi_{;\mu\nu} \phi \\ & + \frac{2}{d} \xi g_{\mu\nu} \phi \square \phi - \xi \left[R_{\mu\nu} - \frac{1}{2} R g_{\mu\nu} + \frac{2(d-1)}{d} \xi R g_{\mu\nu} \right] \phi^2 \\ & + 2 \left[\frac{1}{4} - \left(1 - \frac{1}{d}\right) \xi \right] g_{\mu\nu} m^2 \phi^2 \end{aligned} \quad (3.30)$$

Also we need to do a slight modification for the modes of the Bunch-Davies vacuum. We still have the expression

$$u_{\vec{k}} = \frac{1}{\pi\alpha} \sqrt{\frac{(-\eta)^3}{32}} H_\nu^{(1)}(-k\eta) e^{i\vec{k}\cdot\vec{x}} \quad (3.31)$$

but now we have $\nu^2 = 9/4 - m^2\alpha^2 - \xi R\alpha^2$. We still assume $\nu^2 \geq 0$.

Conformal coupling at the local vacuum

When adding the extra term to the action, we get an extra choice when constructing the local vacuum. When we construct the local vacuum we compare the field to the same field in Minkowski space. But how do we give this Minkowski field the same action? If we add $-\xi R\phi^2$ in Minkowski space, this term vanishes, since in Minkowski space we have no curvature. We could instead choose to fix the Ricci scalar R to the value from our original spacetime.

To include both options in our calculations we change our Minkowski action when constructing the local vacuum to

$$S = \int d^4x \frac{1}{2} (\eta^{\mu\nu} \partial_\mu \phi \partial_\nu \phi - (m^2 + \chi R_0) \phi^2) \quad (3.32)$$

Here R_0 is not the curvature of Minkowski space but from our original curved spacetime. The reasonable values for χ are $\chi = 0$ and $\chi = \xi$, which we will call “without compensation” and “with compensation” respectively.

This modification slightly changes our initial conditions in the construction of the local vacuum (equations (2.21) and (2.22)). To get the corrected version we have to change ω_k .

⁴If we don't want it, we can always remove it by simply setting $\xi = 0$.

This will give

$$u_{\vec{k}}(\eta_0, x^i) = \frac{1}{\sqrt{2(2\pi a_0)^3 \omega_k}} e^{i\vec{k}\cdot\vec{x}} \quad \text{with} \quad \omega_k = \sqrt{m^2 + \chi R_0 + k^2/a_0^2} \quad (3.33)$$

and

$$\dot{u}_{\vec{k}}(\eta_0, x^i) = -i \sqrt{\frac{\omega_k}{2(2\pi)^3 a_0}} e^{i\vec{k}\cdot\vec{x}} \quad (3.34)$$

where R_0 is given by

$$R_0 = 6 \frac{\ddot{a}}{a^3} \Big|_{\eta=\eta_0} \quad (3.35)$$

3.4 Detectors in the Bunch-Davies vacuum

Since the local vacuum is based on the experiences of inertial local observers, it is interesting to see what these observers experience in a Bunch-Davies vacuum.

Let's consider the response function of a simple monopole detector as in equation (1.58):

$$\mathcal{F}(E) = \int_{-\infty}^{\infty} d\tau \int_{-\infty}^{\infty} d\tau' e^{-iE(\tau-\tau')} \langle 0 | \hat{\phi}(x(\tau)) \hat{\phi}(x(\tau')) | 0 \rangle \quad (3.36)$$

It can be shown that in the massless, conformally coupled limit, this reduces for comoving observers to

$$\frac{\mathcal{F}(E)}{\Delta\tau} = \frac{E}{2\pi} \frac{1}{\exp(2\pi\alpha E) - 1} \quad (3.37)$$

Just like the Unruh effect, this is a thermal spectrum, this time with temperature $T = 1/(2\pi\alpha)$. [1]

This means that even inertial particle detectors will detect particles in the Bunch-Davies vacuum. This means that the Bunch-Davies vacuum would be different from the local vacuum. In the next chapter we will compare both states to see how they are related.

Summary

We want to test the local vacuum by comparing it to another vacuum definition. In Minkowski space the local vacuum is trivial, so we switch to de Sitter space. De Sitter space can be defined as a hyperboloid embedded in five-dimensional Minkowski space. We can choose a set of coordinates for one half of the space, such that the metric is a flat FRW-metric. This makes it possible to implement the local vacuum example from the previous chapter.

The de Sitter space is maximally symmetric: it is homogeneous and isotropic. The Ricci scalar is therefore a constant, which turns out to be positive.

We can use all the symmetries of the de Sitter space to determine a splitting in modes that gives a vacuum that is invariant under these symmetries. This gives the Bunch-Davies vacuum.

De Sitter space is related to Minkowski space by a specific conformal transformation, which gives the metric an overall, spacetime-dependent scale factor. If we want to make our physics invariant under these conformal transformations, we need to restrict ourselves to massless fields and we need to add an extra coupling to the Ricci scalar to our action.

We can also include this term in our action for massive fields. This changes some of our formulas. If we include this extra term, we have some freedom for handling the Ricci curvature in this term when we construct the local vacuum and analyse the field in Minkowski space: we can either take the Minkowski curvature, which is zero, (“without compensation”) or we can artificially keep the curvature of our original spacetime (“with compensation”). To include both options we give this term a separate coupling constant χ .

When we put a particle detector in the Bunch-Davies vacuum, it measures in the massless, conformally coupled limit a heat bath of particles, with temperature dependent on the curvature of the de Sitter space. This indicates that the Bunch-Davies vacuum is different from the local vacuum.

Chapter 4

Comparison Local and Bunch-Davies vacuum

In the previous chapters we showed that when we consider Quantum Field Theory in curved spacetimes, we have an ambiguity when defining a vacuum state. We also introduced the local vacuum, which can circumvent this ambiguity by only being a special state locally. To test the local vacuum we are going to compare it to the Bunch-Davies vacuum in de Sitter space, which we introduced in the last chapter.

In the first section we will discuss how we do the comparison and the role of regularisation. In the second and third section we do the comparison using cutoff and dimensional regularisation respectively. In the fourth section we will interpret these results.

In the fifth section we will compare both the local vacuum and the Bunch-Davies vacuum to a numerical simulation.

For readability, some of the calculations have been moved to appendices B and C.

4.1 UV-divergence

Before we can do the comparison between our two states, we first need to determine how we will compare the two states. We need some physical quantity that we can compare. Since the local vacuum is only a special state locally, we preferably use a local quantity.

A reasonable choice will be to use the expectation value of the stress energy tensor. As we saw in section 1.2, the stress energy tensor is an important quantity when doing a semi-classical approach. Mayor differences in the expectation value of the stress energy tensor therefore also indicate mayor differences in the states. This makes the stress energy tensor a good quantity to compare.

We will also need to look at the divergences in these expectation values. In chapter 1 we saw that the energy density of the Minkowski vacuum has a UV-divergence: the contribution of large wavenumbers to the energy density is giving a diverging expression.

The same thing is happening for the stress energy tensor in de Sitter space. We will get diverging expectation values due to the contribution of high wavenumbers. This is clearly unphysical: we would for example get an infinite contribution in the Einstein equations (1.60).

To make sense of the diverging expectation value, we need renormalisation. We can add some terms in the action that will exactly compensate the divergence. Then only the finite, physical parts will remain. For the renormalisation of the stress energy tensor for the Bunch-Davies vacuum, see [1].

These divergence-compensating terms are independent of the state, so they are the same for the local vacuum and the Bunch-Davies vacuum. This means that if we take the difference between the expectation values in both states, we expect something that is independent of the compensating terms. So this difference is the same before and after renormalisation.

We are interested in the differences between the local vacuum and the Bunch-Davies vacuum after renormalisation, but clearly we can just take the difference before renormalisation.

Of course we need to be very careful when taking the difference between two diverging expressions. To do this properly, we have to do regularisation: we introduce a parameter that makes our expression finite (we regulate it), until we take a certain limit, which gives our original, diverging expression. The finite, regulated expressions can be subtracted from each other without problems. After that we can take the limit of our parameter. If this gives a converging difference, we have got our difference of the diverging expressions. If this divergences, our diverging expressions will have a diverging difference, even after renormalisation.

In principle, it should not matter which regularisation method we choose. Each method has its advantages and disadvantages. We will use both cutoff regularisation and dimensional regularisation in the next two sections.

As we will see shortly, the difference between the expectation values of the stress energy tensor in the local vacuum and the Bunch-Davies vacuum will not converge in most cases. Since this issue needs to be resolved before we can make sense of the finite parts, we will neglect the finite parts of the difference in this thesis.

4.2 Cutoff regularisation

Our first regularisation method is quite intuitive. The divergences in our expressions arise when we include large wavenumbers. To regularise this, we introduce a maximal value for the wavenumber, k_{\max} . We can restore our diverging expressions by taking the limit $k_{\max} \rightarrow \infty$.

In practice, we change the bounds of our integrals, for example in our field operator (1.27). We make the following changes:

$$\int d^3k = \int d\Omega \int_0^\infty dk k^2 \mapsto \int d\Omega \int_0^{k_{\max}} dk k^2 \quad (4.1)$$

As we show in the full computations in appendix B, there is no IR-divergence (for $k \rightarrow 0$). This means that if we move the lower bound of our integral to an arbitrary value k_0 , we only change the outcome by a finite amount. Since we are not yet interested in the finite parts, we can neglect this. The integral becomes

$$\int d\Omega \int_{k_0}^{k_{\max}} dk k^2 \quad (4.2)$$

We can take k_0 to be arbitrarily high. Since we are only integrating over arbitrarily high values of k we can replace difficult expressions like $H_\nu^{(1)}(-k\eta_0)$ by their asymptotics for high k .

In appendix B, we show that we get the following expectation values for \hat{T}_{00} :

$$\begin{aligned} \langle \hat{T}_{00} \rangle_{BD} = & \frac{1}{4\pi^2\alpha^4} a_0^2 \int_{z_0}^{z_{\max}} dz \left[z^3 + z \frac{m^2\alpha^2 - 6(\xi - 1/6)}{2} \right. \\ & \left. - \frac{m^2\alpha^2(m^2\alpha^2 + 12(\xi - 1/6))}{8z} \right] + \text{regular terms} \end{aligned} \quad (4.3)$$

$$\begin{aligned} \langle \hat{T}_{00} \rangle_L = & \frac{1}{4\pi^2\alpha^4} a_0^2 \int_{z_0}^{z_{\max}} dz \left[z^3 + z \frac{m^2\alpha^2 + 6\xi}{2} \right. \\ & \left. - \frac{(m^2\alpha^2 + 12\chi)(m^2\alpha^2 + 12(\xi - \chi))}{8z} \right] + \text{reg.} \end{aligned} \quad (4.4)$$

$$\begin{aligned} \langle \hat{T}_{00} \rangle_L - \langle \hat{T}_{00} \rangle_{BD} = & \frac{1}{4\pi^2\alpha^4} a_0^2 \int_{z_0}^{z_{\max}} dz \left[z \frac{12\xi - 1}{2} - \frac{m^2\alpha^2 + 72\chi(\xi - \chi)}{4z} \right] \\ & + \text{regular terms} \end{aligned} \quad (4.5)$$

Where we have substituted $z = -\eta_0 k$. For $z_{\max} \rightarrow \infty$, we see that the difference between the two expectation values diverges for any combination of ξ and χ . The quartic divergence¹ always cancels, but at least the logarithmic divergence remains.

¹The z^3 -term integrated gives z_{\max}^4 and therefore is called quartic. The z - and z^{-1} -terms give z_{\max}^2 and $\ln(z_{\max})$, and are called quadratic and logarithmic respectively.

Similarly, for \hat{T}_{ii} we get

$$\begin{aligned} \langle \hat{T}_{ii} \rangle_{BD} = \frac{1}{4\pi^2\alpha^4} a_0^2 \int_{z_0}^{z_{\max}} dz \left[\frac{z^3}{3} + z \frac{-m^2\alpha^2 + 6(\xi - 1/6)}{6} \right. \\ \left. + \frac{m^2\alpha^2(m^2\alpha^2 + 12(\xi - 1/6))}{8z} \right] + \text{reg.} \end{aligned} \quad (4.6)$$

$$\begin{aligned} \langle \hat{T}_{ii} \rangle_L = \frac{1}{4\pi^2\alpha^4} a_0^2 \int_{z_0}^{z_{\max}} dz \left[\frac{z^3}{3} + z \frac{-m^2\alpha^2 + 24\xi(6\xi - 6\chi - 3/4) + 24\chi}{6} \right. \\ \left. + \frac{(m^2\alpha^2 + 12\chi)(m^2\alpha^2 - 12(8\xi - 1)(\xi - \chi))}{8z} \right] + \text{reg.} \end{aligned} \quad (4.7)$$

$$\begin{aligned} \langle \hat{T}_{ii} \rangle_L - \langle \hat{T}_{ii} \rangle_{BD} = \frac{1}{4\pi^2\alpha^4} a_0^2 \int_{z_0}^{z_{\max}} dz \left[z \frac{1 + 24(6\xi - 1)(\xi - \chi)}{6} \right. \\ \left. + \frac{m^2\alpha^2(1 - 48\xi(\xi - \chi)) - 72\chi(8\xi - 1)(\xi - \chi)}{4z} \right] + \text{reg.} \end{aligned} \quad (4.8)$$

Again the quartic divergence cancels. The other divergences also cancel for the combination $\xi = 1/8$ and $\chi = -1/24$. However, since these are not expected values for ξ and χ , and they don't show up for expectation values of \hat{T}_{00} , we don't know whether this is something physical (or is pointing us to something physical) or just coincidence.

Also note that for both $\langle \hat{T}_{00} \rangle$ and $\langle \hat{T}_{ii} \rangle$ all divergences cancel when we take $\xi = 1/6$ for the Bunch-Davies vacuum, but $\xi = \chi = 0$ for the local vacuum.

Note that, even for the symmetrical Bunch-Davies vacuum, the stress energy tensor in this regularisation is not proportional to the metric. This is not a property of the vacuum, but an artefact of the cutoff regularisation method.

We introduced a cutoff in k , which is related to our spatial coordinates. This cutoff implies a different cutoff in ω_k , which is related to the time coordinate. This means that the cutoff treats time and space differently, so it breaks the symmetry between time and space. Only after renormalisation, we expect to retrieve the spacetime symmetry in the Bunch-Davies vacuum.

The dimensional regularisation in the next section does preserve the symmetry during the regularisation.

Finally, we can look at the trace of the stress-energy tensor $\hat{T} = \hat{T}^\mu_\mu$:

$$\begin{aligned} \langle \hat{T} \rangle_{BD} = \frac{1}{4\pi^2\alpha^4} \int_{z_0}^{z_{\max}} dz & \left[z(m^2\alpha^2 - 6(\xi - 1/6)) \right. \\ & \left. - \frac{m^2\alpha^2(m^2\alpha^2 + 12(\xi - 1/6))}{2z} \right] + \text{reg.} \end{aligned} \quad (4.9)$$

$$\begin{aligned} \langle \hat{T} \rangle_L = \frac{1}{4\pi^2\alpha^4} \int_{z_0}^{z_{\max}} dz & \left[z(m^2\alpha^2 - 72(\xi - 1/6)(\xi - \chi)) \right. \\ & \left. - \frac{(m^2\alpha^2 + 12\chi)(m^2\alpha^2 - 72(\xi - 1/6)(\xi - \chi))}{2z} \right] + \text{reg.} \end{aligned} \quad (4.10)$$

$$\begin{aligned} \langle \hat{T} \rangle_L - \langle \hat{T} \rangle_{BD} = \frac{1}{4\pi^2\alpha^4} \int_{z_0}^{z_{\max}} dz & \left[-72z(\xi - 1/6)(\xi - \chi - 1/12) \right. \\ & \left. - \frac{m^2\alpha^2(1 - 36\xi(\xi - \chi)) - 72\chi(6\xi - 1)(\xi - \chi)}{z} \right] + \text{reg.} \end{aligned} \quad (4.11)$$

Note that this last expression converges for $\xi = 1/6$ and $\chi = 0$, which is the case for conformal coupling without compensation in Minkowski space.

For an overview of the results using the expected combinations of ξ and χ , see table 4.1 on page 42.

4.3 Dimensional regularisation

Our second regularisation method might be less intuitive, but has the nice advantage that it preserves the spacetime symmetry.

In dimensional regularisation, we change the number of spacetime dimensions to a variable d . We keep one time dimension, so the number of spatial dimensions becomes $d - 1$. We can restore the diverging limit by taking $d \rightarrow 4$ or by defining $\epsilon = 4 - d$ and taking $\epsilon \rightarrow 0$.

Preferably, our expressions converge for all $d \neq 4$, but unfortunately our expressions diverge for all d . That is why we need to do an extra trick involving analytical continuation.

Consider the following integral:

$$\int_0^1 dz z^{a-1} (1-z)^{b-1} \quad (4.12)$$

For $\text{Re}(a) > 0$ and $\text{Re}(b) > 0$ this integral converges: [5]

$$\int_0^1 dz z^{a-1} (1-z)^{b-1} = \frac{\Gamma(a)\Gamma(b)}{\Gamma(a+b)} \quad [\text{Re}(a) > 0 \quad \text{and} \quad \text{Re}(b) > 0] \quad (4.13)$$

We will encounter this integral where at least one of the parameters has a negative real part. Formally the integral diverges in this case, but we can assign it

to the analytical continuation of the right hand side of equation (4.13). In this step we implicitly remove a divergence, without bothering how it is renormalised.

In appendix C, we show that we get the following expectation values for \hat{T}_{00} :

$$\langle \hat{T}_{00} \rangle_{BD} = -\frac{m^2\alpha^2(m^2\alpha^2 + 12(\xi - 1/6))}{32\pi^2\alpha^4} a_0^2(1/\epsilon + \mathcal{O}(\epsilon^0)) \quad (4.14)$$

$$\langle \hat{T}_{00} \rangle_L = -\frac{(m^2\alpha^2 + 12\chi)(m^2\alpha^2 + 12(\xi - \chi))}{32\pi^2\alpha^4} a_0^2(1/\epsilon + \mathcal{O}(\epsilon^0)) \quad (4.15)$$

$$\langle \hat{T}_{00} \rangle_L - \langle \hat{T}_{00} \rangle_{BD} = -\frac{m^2\alpha^2 + 72\chi(\xi - \chi)}{16\pi^2\alpha^4} a_0^2(1/\epsilon + \mathcal{O}(\epsilon^0)) \quad (4.16)$$

For any combination of ξ and χ the difference diverges when taking the limit $\epsilon \rightarrow 0$.

For \hat{T}_{ii} , we get:

$$\langle \hat{T}_{ii} \rangle_{BD} = \frac{m^2\alpha^2(m^2\alpha^2 + 12(\xi - 1/6))}{32\pi^2\alpha^4} a_0^2(1/\epsilon + \mathcal{O}(\epsilon^0)) \quad (4.17)$$

$$\langle \hat{T}_{ii} \rangle_L = \frac{(m^2\alpha^2 + 12\chi)(m^2\alpha^2 - 12(8\xi - 1)(\xi - \chi))}{32\pi^2\alpha^4} a_0^2(1/\epsilon + \mathcal{O}(\epsilon^0)) \quad (4.18)$$

$$\langle \hat{T}_{ii} \rangle_L - \langle \hat{T}_{ii} \rangle_{BD} = \frac{m^2\alpha^2(1 - 48\xi(\xi - \chi)) - 72\chi(8\xi - 1)(\xi - \chi)}{16\pi^2\alpha^4} a_0^2(1/\epsilon + \mathcal{O}(\epsilon^0)) \quad (4.19)$$

The divergence here cancels again for the combination $\xi = 1/8$ and $\chi = -1/24$, which we also saw for the cutoff regularisation, but now also for $\xi = \sqrt{1/48}$ and $\chi = 0$. Unfortunately, this result does not seem quite physical.

Note that the expressions in the dimensional regularisation case exactly match the logarithmic divergences for the cutoff regularisation. It's therefore no surprise that also now holds that for both \hat{T}_{00} and \hat{T}_{ii} , the divergences cancel when we take $\xi = 1/6$ for the Bunch-Davies vacuum, but $\xi = \chi = 0$ for the local vacuum.

We can see that the Bunch-Davies vacuum is symmetric ($\langle \hat{T}_{\mu\nu} \rangle$ is proportional to $g_{\mu\nu}$), as we would expect. Note that the local vacuum is only symmetric for $\xi = 0$ or $\chi = \xi$.

We can again look at the trace of the stress energy tensor:

$$\langle \hat{T} \rangle_{BD} = -\frac{m^2\alpha^2(m^2\alpha^2 + 12(\xi - 1/6))}{8\pi^2\alpha^4} (1/\epsilon + \mathcal{O}(\epsilon^0)) \quad (4.20)$$

$$\langle \hat{T} \rangle_L = -\frac{(m^2\alpha^2 + 12\chi)(m^2\alpha^2 - 72(\xi - 1/6)(\xi - \chi))}{8\pi^2\alpha^4} (1/\epsilon + \mathcal{O}(\epsilon^0)) \quad (4.21)$$

$$\langle \hat{T} \rangle_L - \langle \hat{T} \rangle_{BD} = -\frac{m^2\alpha^2(1 - 36\xi(\xi - \chi)) - 72\chi(6\xi - 1)(\xi - \chi)}{4\pi^2\alpha^4} (1/\epsilon + \mathcal{O}(\epsilon^0)) \quad (4.22)$$

Note that this last expression converges again for $\xi = 1/6$ and $\chi = 0$.

For an overview of the results using the expected combinations of ξ and χ , see table 4.2 on page 43.

We evaluate the expectation values around the pole at $d = 4$, since this is physically most interesting, but note that we also have poles at $d = 0, 2, 6, 8, \dots$. Using the results from appendix C, it is not hard to show that around the pole at $d = 2$ we do not have divergent differences between the Bunch-Davies vacuum and the local vacuum for $\xi = 0$ or for $\chi = \xi$.²

4.4 Interpretation

How should we look at these results? Firstly, let's note that the results of both regularisation methods are fairly consistent. Within the expected values of ξ and χ there is no combination to get a convergent difference in the stress energy tensor expectation values. When we take conformal coupling without compensation, the difference in the expectation values of the trace does converge. This is true in both methods.

The consistency is even more clear if we only look at the logarithmic divergences in the cutoff regularisation. The parameters in this divergence exactly match the parameters in the dimensional regularisation. This immediately raises the question how we should look at the quadratic divergences we often have in the cutoff regularisation. Either they are physical (but then why don't they show up in the dimensional regularisation?) or they are an artefact of the violation of symmetry when doing the cutoff (note that these terms are not symmetric in the Bunch-Davies vacuum).

When we use the dimensional regularisation, we preserve the spacetime symmetry and we see that the expectation values in the Bunch-Davies vacuum are neatly symmetric. Interestingly, the local vacuum only has this symmetry when we have minimal coupling or when we do the compensation in Minkowski space.

On the other hand, when we have conformal coupling without compensation, we don't have the spacetime symmetry in the local vacuum, but we do have a matching value of the trace of the stress energy tensor, which is a scalar quantity.

We could interpret these diverging differences as an ideal gas with infinite energy density. If we look at the ratio between the expectation values of \hat{T}_{00} and \hat{T}_{ii} , we can determine what kind of ideal gas we have.[4] We only consider the dimensional regularisation for this purpose, since it preserves the spacetime symmetry. In that case we see that the ideal gas that gives the diverging difference is a vacuum energy (ratio of -1) for $\xi = \chi = 0$ and $\xi = \chi = 1/6$, but can be seen as radiation (ratio of 1/3) for $\xi = 1/6$ and $\chi = 0$.

²Note that for $d = 2$ the conformal coupling is also given by $\xi = 0$.

Table 4.1: A short overview of the differences of some stress energy expectation values between the local vacuum and the Bunch-Davies vacuum, for the expected combinations of ξ and χ , using cutoff regularisation. Note that only in one case we have a converging difference, i.e. for the trace of the stress energy tensor, with conformal coupling and without compensation.

NB: To shorten the table we only display $f(z)$ defined by:

$$\langle \hat{A} \rangle_L - \langle \hat{A} \rangle_{BD} = \frac{1}{4\pi^2\alpha^4} a_0^2 \int_{z_0}^{z_{\max}} dz f(z) + \text{regular terms}$$

$\xi = \chi = 0$	
$\hat{A} = \hat{T}_{00} :$	$f(z) = -\frac{z}{2} - \frac{m^2\alpha^2}{4z}$
$\hat{A} = \hat{T}_{ii} :$	$f(z) = \frac{z}{6} + \frac{m^2\alpha^2}{4z}$
$\hat{A} = \hat{T} :$	$f(z) = a_0^{-2} \left[-z - \frac{m^2\alpha^2}{z} \right]$
$\xi = 1/6 \quad \chi = 0$	
$\hat{A} = \hat{T}_{00} :$	$f(z) = \frac{z}{2} - \frac{m^2\alpha^2}{4z}$
$\hat{A} = \hat{T}_{ii} :$	$f(z) = \frac{z}{6} - \frac{m^2\alpha^2}{12z}$
$\hat{A} = \hat{T} :$	$f(z) = 0$
$\xi = \chi = 1/6$	
$\hat{A} = \hat{T}_{00} :$	$f(z) = \frac{z}{2} - \frac{m^2\alpha^2}{4z}$
$\hat{A} = \hat{T}_{ii} :$	$f(z) = \frac{z}{6} + \frac{m^2\alpha^2}{4z}$
$\hat{A} = \hat{T} :$	$f(z) = a_0^{-2} \left[-\frac{m^2\alpha^2}{z} \right]$

Table 4.2: A short overview of the differences of some stress energy expectation values between the local vacuum and the Bunch-Davies vacuum, for the expected combinations of ξ and χ , using dimensional regularisation. Note that only in one case we have a converging difference, i.e. for the trace of the stress energy tensor, with conformal coupling and without compensation.

NB: To shorten the table we only display q defined by:

$$\langle \hat{A} \rangle_L - \langle \hat{A} \rangle_{BD} = \frac{q}{16\pi^2\alpha^4} a_0^2 (1/\epsilon + \mathcal{O}(\epsilon^0))$$

$\xi = \chi = 0$	
$\hat{A} = \hat{T}_{00} :$	$q = -m^2\alpha^2$
$\hat{A} = \hat{T}_{ii} :$	$q = m^2\alpha^2$
$\hat{A} = \hat{T} :$	$q = a_0^{-2}[-4m^2\alpha^2]$
$\xi = 1/6 \quad \chi = 0$	
$\hat{A} = \hat{T}_{00} :$	$q = -m^2\alpha^2$
$\hat{A} = \hat{T}_{ii} :$	$q = -\frac{m^2\alpha^2}{3}$
$\hat{A} = \hat{T} :$	$q = 0$
$\xi = \chi = 1/6$	
$\hat{A} = \hat{T}_{00} :$	$q = -m^2\alpha^2$
$\hat{A} = \hat{T}_{ii} :$	$q = m^2\alpha^2$
$\hat{A} = \hat{T} :$	$q = a_0^{-2}[-4m^2\alpha^2]$

4.5 Simulations

In the last sections we saw that there is a diverging energy difference between the local vacuum and the Bunch-Davies vacuum. Since it is a difference, it should even remain after renormalisation. Having diverging quantities after renormalisation has quite some consequences (the infinite energy density would e.g. have an infinite back-reaction on the curvature of the spacetime) and would therefore be unphysical. This means that (at least) one of our vacua is an unphysical state. In this section we try to determine which one is unphysical.

To do this, we start with the Minkowski vacuum in Minkowski space, since we have seen that this vacuum is unambiguous. Then, we smoothly change the scale factor $a(\eta)$ of our spacetime to transition from Minkowski space to the de Sitter space (see figure 4.1). We make sure that the scale factor and its derivative are continuous everywhere. This transition, although smoothly, could lead to particle creation, so we might end up in a non-vacuum state, but since the transition is smooth and for a finite time, we assume that we only get finite energy differences with respect to a physical vacuum.

We start with the modes of the Minkowski vacuum and, using the Klein-Gordon equation, we numerically let the modes evolve in the transition region.³ We use the resulting modes to numerically determine the stress energy tensor in this simulated state and compare it to the stress energy tensors in the Bunch-Davies and local vacuum.

We still have to use a regularisation method to be able to compare the divergent expressions. We will use the cutoff regularisation from section 4.2. We will also use notation comparable to table 4.1: we only consider $f(z)$ defined by

$$\langle \hat{A} \rangle_i - \langle \hat{A} \rangle_{\text{simul.}} = \frac{1}{4\pi^2\alpha^4} a_0^2 \int_{z_0}^{z_{\text{max}}} dz f(z) \quad (4.23)$$

where \hat{A} is one of the stress energy tensor components or its trace and the subscript i indicates either the local vacuum or the Bunch-Davies vacuum.

We chose the following parameters: $m = 1/16$, $\alpha = 4$ (so $m^2\alpha^2 < 1/4$) and $\eta_0 = -2.5$. We plotted the different $f(z)$ on a log-log scale to see the power law behaviour. The plots are given in figures 4.2, 4.3 and 4.4.

In figures 4.3 and 4.4 we can see that the simulations with conformal coupling do correspond nicely with the Bunch-Davies vacuum (yellow squares). We see a descending slope with slope smaller than -1, so the integral over $f(z)$ is convergent. The slope only rises when we get close to the order of magnitude of the rounding errors. Since in that case the points also don't align properly and sometimes switch sign, we can safely assume that this rising is indeed due to the rounding error in the simulations.

We see in figure 4.2 that the Bunch-Davies vacuum at minimal coupling does not quite correspond with the simulation. In \hat{T}_{00} we see roughly a linear

³The solutions of the Klein-Gordon equations should remain normalised. Due to numerical errors the modes in the simulations slightly shifted from their normalisation. At the boundary between the transition region and the de Sitter space ($\eta = -3$) and before computing the stress energy tensor, the normalisation of the modes was restored.

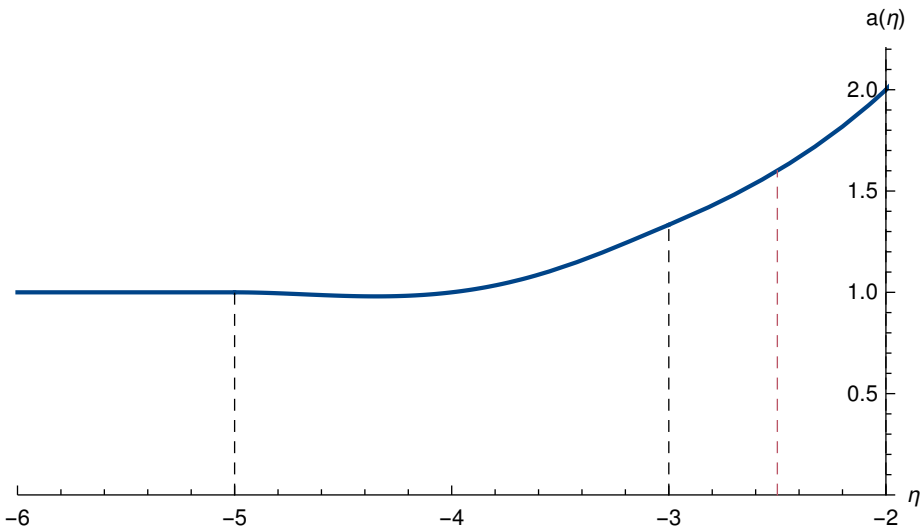


Figure 4.1: The scalefactor $a(\eta)$ of the universe of the simulations. We start in Minkowski space at $\eta < -5$ and make a smooth transition to de Sitter space which starts at $\eta = -3$. At the red line at $\eta = -2.5$ we evaluate the expectation value of the stress energy tensor in this simulation and for the two vacua.

(slope of 0) and a cubic (slope of 2) divergence remaining and we see a roughly quadratic divergence for the other components. The fact that the data is not properly aligned and often switches sign makes it hard to determine whether these divergences are physical (e.g. due to some oscillating behaviour in z) or an artefact of the simulations, although we are clearly above the rounding errors.

Since the Bunch-Davies vacuum corresponds with the simulations with conformal coupling, we expect (according to table 4.1) that the local vacuum has diverging differences with respect to the simulations, except for the trace of the stress energy tensor when we have $\chi = 0$. The results in figures 4.3 and 4.4 confirm this. We can clearly see the expected divergences (and one convergence) with the right signs.

At minimal coupling, the local vacuum also doesn't correspond with the simulations. For \hat{T}_{00} we see a clear sharp quadratic divergence, in the other cases we see the same rough quadratic divergence as with the Bunch-Davies vacuum. For \hat{T}_{00} the divergence is clear enough to say that it is probably not an artefact of the simulations. In the other cases it is hard to interpret the result, as we saw for the Bunch-Davies vacuum.

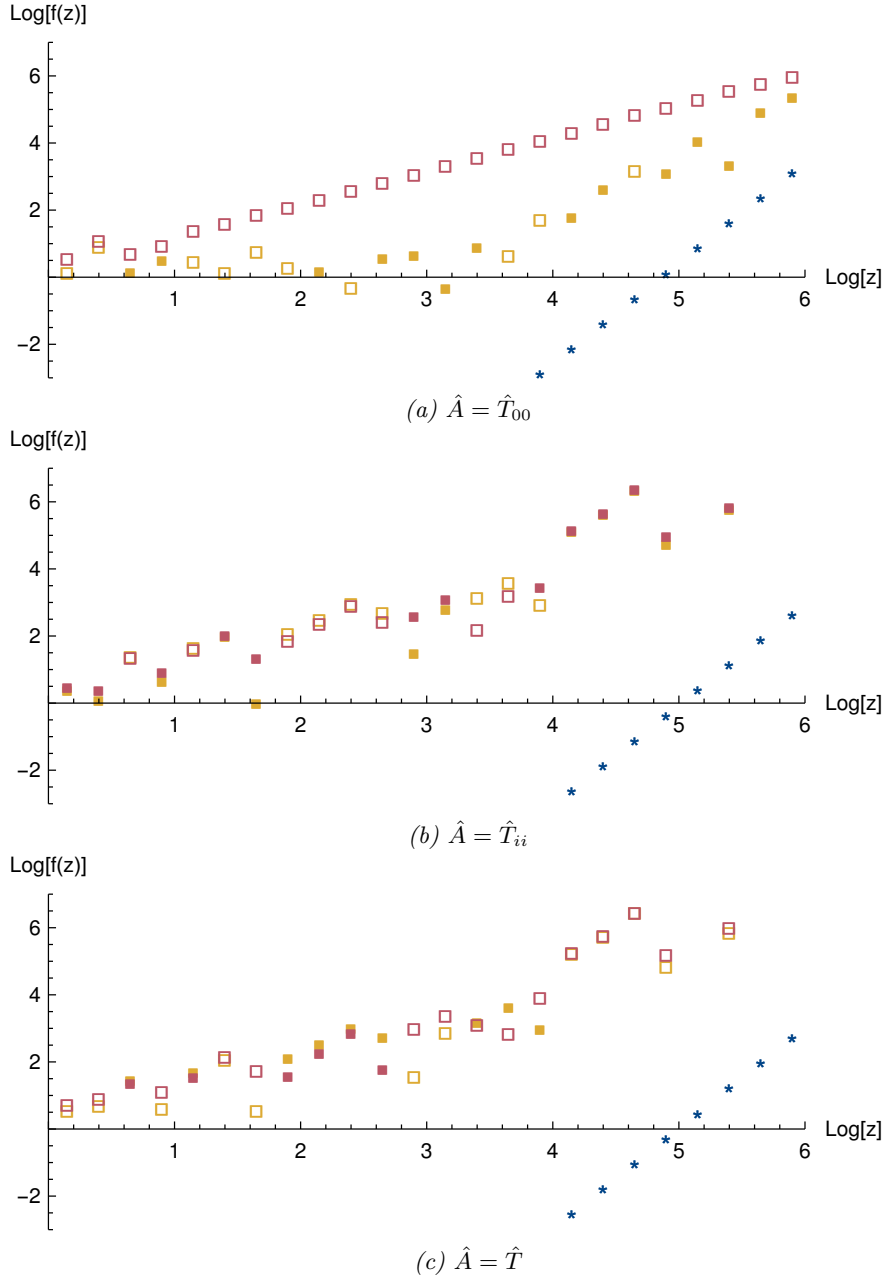


Figure 4.2: The difference between the two vacua and the simulation regarding the expectation values of a stress energy tensor component or its trace. The function $f(z)$ is defined in equation (4.23).

The red squares indicate the differences between the local vacuum and the simulated state, the yellow squares indicate the differences between the Bunch-Davies vacuum and the simulated state. Open squares indicate that the difference is negative. The blue stars indicate the order of magnitude of the rounding errors in the simulation.

These 3 plots correspond to the **minimal coupling** ($\xi = \chi = 0$). Other couplings can be found in figures 4.3 and 4.4.

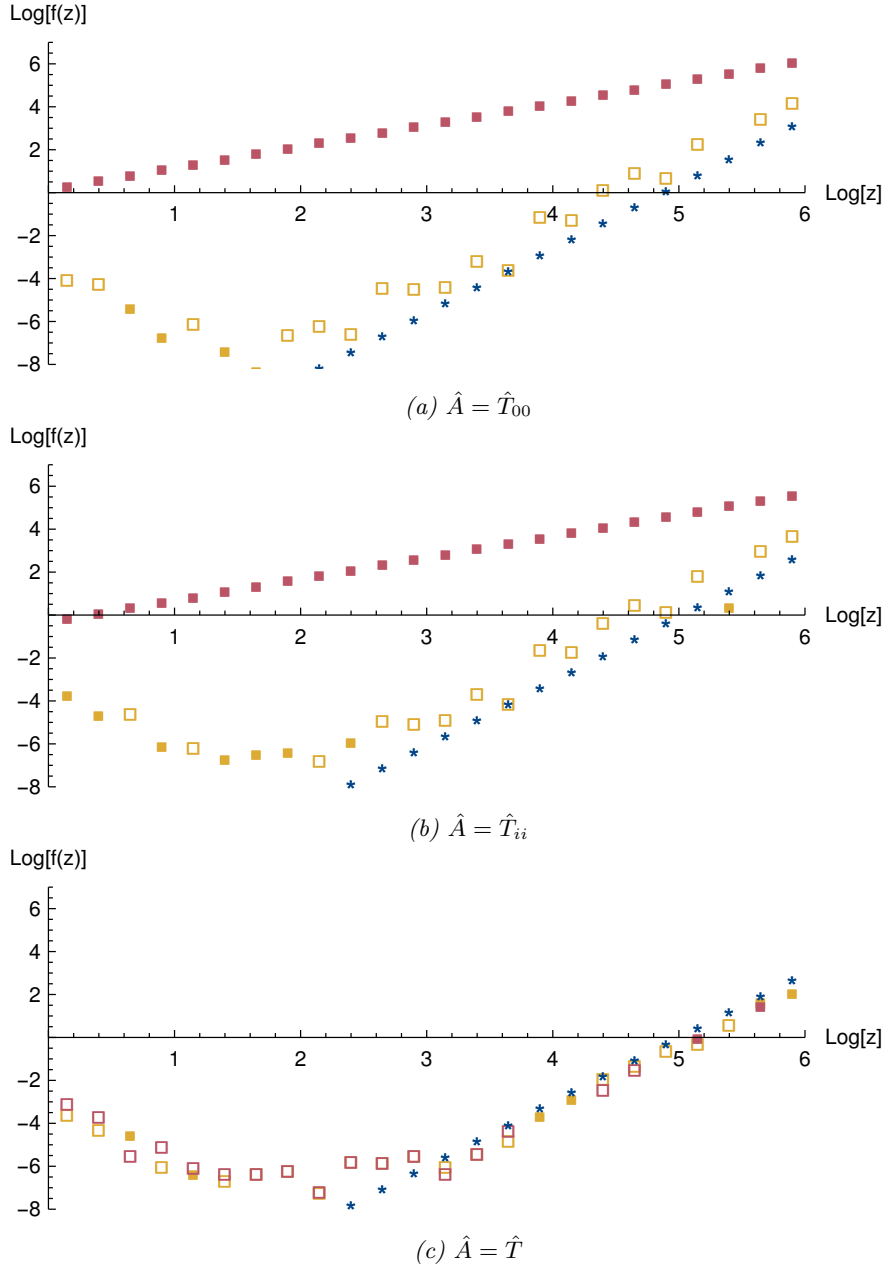


Figure 4.3: The difference between the two vacua and the simulation regarding the expectation values of a stress energy tensor component or its trace. The function $f(z)$ is defined in equation (4.23).

The red squares indicate the differences between the local vacuum and the simulated state, the yellow squares indicate the differences between the Bunch-Davies vacuum and the simulated state. Open squares indicate that the difference is negative. The blue stars indicate the order of magnitude of the rounding errors in the simulation.

These 3 plots correspond to the **conformal coupling without compensation** ($\xi = 1/6$, $\chi = 0$). Other couplings can be found in figures 4.2 and 4.4.

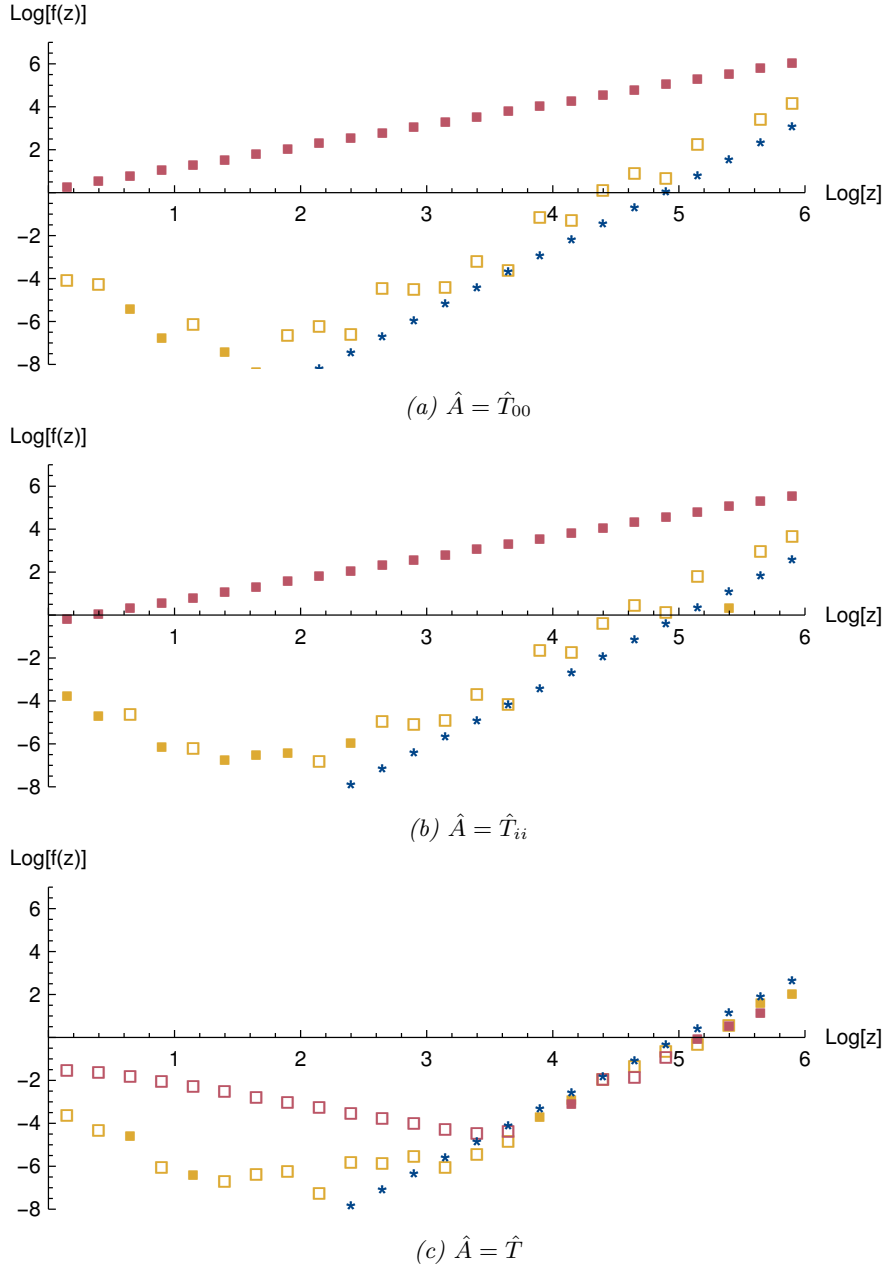


Figure 4.4: The difference between the two vacua and the simulation regarding the expectation values of a stress energy tensor component or its trace. The function $f(z)$ is defined in equation (4.23).

The red squares indicate the differences between the local vacuum and the simulated state, the yellow squares indicate the differences between the Bunch-Davies vacuum and the simulated state. Open squares indicate that the difference is negative. The blue stars indicate the order of magnitude of the rounding errors in the simulation.

These 3 plots correspond to the **conformal coupling with compensation** ($\xi = \chi = 1/6$). Other couplings can be found in figures 4.2 and 4.3.

To better understand the unexpected behaviour at minimal coupling we have run the same simulation, but now with a much smoother scale factor: all derivatives up to the sixth derivative $\frac{d^6}{d\eta^6}a(\eta)$ are now continuous. The results are shown in figure 4.5.

Note that for the Bunch-Davies vacuum the rough linear divergence in \hat{T}_{00} and the rough quadratic divergence in the other components get reduced, but still a rough cubic and rough quartic divergence remain respectively.

So while the discontinuity of the second derivative of the scale factor was a reason for some of the unexpected divergences at minimal coupling, it can not fully explain all divergences.

Interestingly, at conformal coupling the results hardly change when the scale factor is more smooth.⁴

⁴These results are not shown, because they are hardly different from figures 4.3 and 4.4.

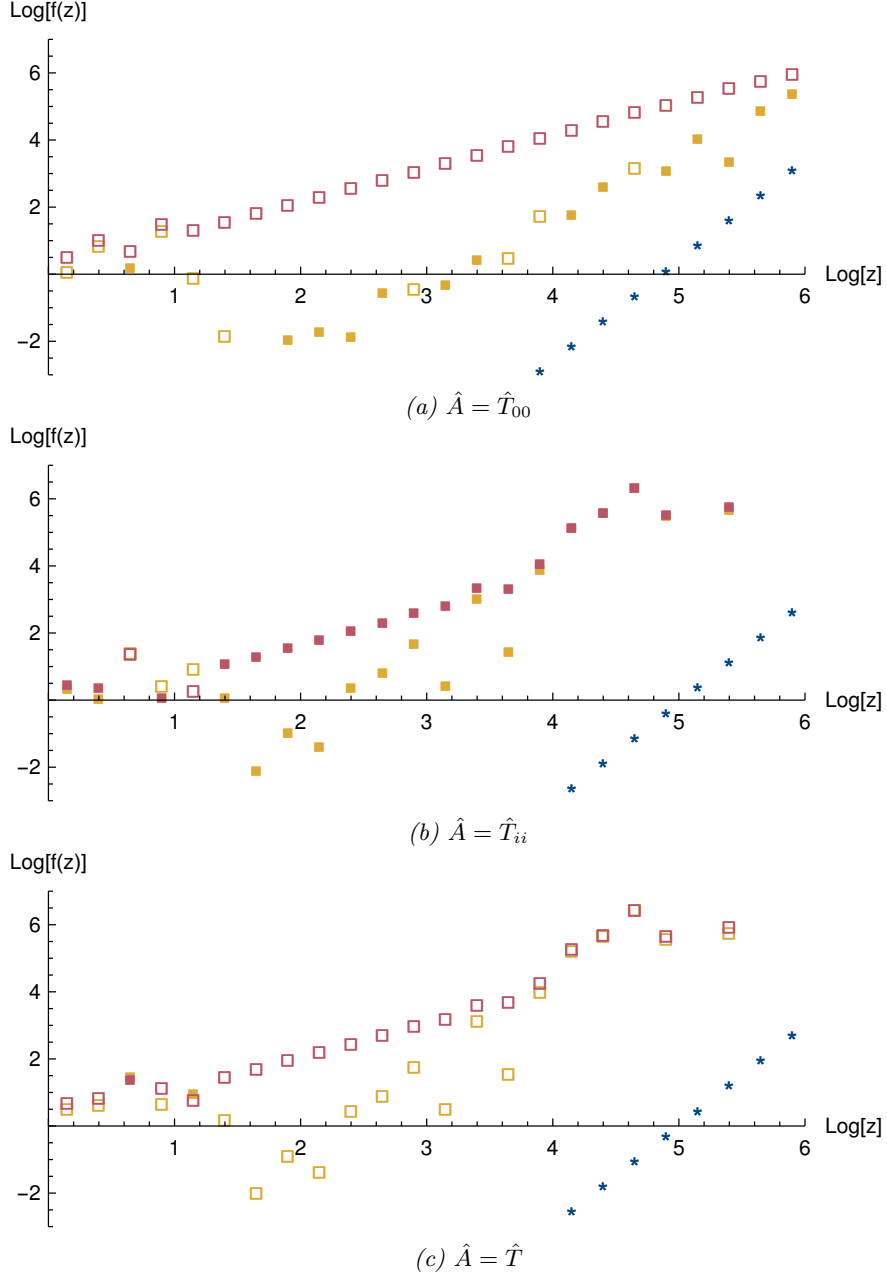


Figure 4.5: The difference between the two vacua and the simulation regarding the expectation values of a stress energy tensor component or its trace. The function $f(z)$ is defined in equation (4.23).

The red squares indicate the differences between the local vacuum and the simulated state, the yellow squares indicate the differences between the Bunch-Davies vacuum and the simulated state. Open squares indicate that the difference is negative. The blue stars indicate the order of magnitude of the rounding errors in the simulation.

These 3 plots correspond to the **minimal coupling** ($\xi = \chi = 0$) and uses a much smoother transition than the results in figure 4.2.

Summary

We compare the local vacuum and the Bunch-Davies vacuum by comparing the expectation values of the stress energy tensor. These expectation values are diverging and need renormalisation to give finite results. The compensation done by the renormalisation is independent on the state, so it is the same for the local vacuum and the Bunch-Davies vacuum. Therefore we can consider the difference between the expectation values of both states before renormalisation, since it will match the difference after renormalisation.

To properly compute the difference between two diverging expressions, we need regularisation. We use two regularisation methods: cutoff regularisation and dimensional regularisation. In the case of cutoff regularisation we impose a maximum value for the wavenumber and take the limit of that maximum to infinity. In the case of dimensional regularisation we change the number of spacetime dimensions and take the limit of this number to four. We also need an analytical continuation, since the expectation values do not converge for any dimension.

We take the difference between the expectation value of the stress energy tensor in the local vacuum and in the Bunch-Davies vacuum. This difference does not converge for both minimal coupling and conformal coupling.

Using cutoff regularisation, we can get a convergent difference if we only consider the spatial components of the stress energy tensor and have a specific value of the coupling to gravity ξ that does not match minimal nor conformal coupling, combined with an unexpected value for the compensation coupling χ . Using dimensional regularisation, there are two such combinations of ξ and χ .

If we only consider the trace of the stress energy tensor, we get a convergent difference for conformal coupling without compensation.

Interestingly, the parameters of the divergence with dimensional regularisation match the parameters of the logarithmic divergence of the cutoff regularisation, but neglect the quadratic divergence. This raises the question whether this quadratic divergence is real or an artefact of the chosen regularisation method.

Furthermore, dimensional regularisation preserves the spacetime symmetry. We can see that the local vacuum only has the full symmetry if we have minimal coupling or compensation in Minkowski space.

If we interpret the diverging differences as contributions from ideal gasses we can determine the type of gas. For minimal coupling and conformal coupling with compensation, this is vacuum energy. For the conformal coupling without compensation, this is radiation.

To see which vacuum is physical (and which one is not), we do a simulation where we start with the Minkowski vacuum in Minkowski space. We do a smooth numerical transition to de Sitter space and compare this data to the local vacuum and the Bunch-Davies vacuum.

We see a clear match with the Bunch-Davies vacuum when we have conformal coupling, while the local vacuum has divergences (except when we only look at the trace of the stress energy tensor and consider conformal coupling without compensation).

When we have minimal coupling neither the local vacuum nor the Bunch-

Davies vacuum matches the simulation, but the differences don't behave smoothly and are therefore hard to interpret. The unexpected behaviour for the Bunch-Davies vacuum can be slightly reduced by making the transition of the scale factor more smooth.

Chapter 5

Conclusion and Outlook

5.1 The local vacuum

The definition of the local vacuum, based on the experiences of local inertial observers, is still flawed.¹ As we have seen in de Sitter space, the local vacuum can be an unphysical state in curved spacetimes, since it has an infinite stress energy tensor compared to physical states, even after renormalisation.

This unphysicality occurs both when we have minimal coupling and conformal coupling of the scalar field.

Furthermore, when we have conformal coupling, the stress energy tensor is not proportional to the metric in the local vacuum. So while being defined in the symmetric de Sitter space, the local vacuum is not symmetric in this case. This means that the construction of the local vacuum creates a preferred time direction.

Interestingly, the trace of the stress energy tensor, which is a scalar and therefore not influenced by the preferred time direction, is in this case finite after renormalisation. This might indicate that only the breaking of the spacetime symmetry is causing problems and that all expectation values of scalar operators are physical in the local vacuum. This is something that could be checked in the future, for example by choosing another scalar operator.

The creation of a preferred time direction can be avoided by applying a specific compensation during the construction of the local vacuum. This makes the local vacuum symmetric again, but unfortunately it also breaks the convergent difference with physical states regarding the expectation value of the trace of the stress energy tensor. We could say that the compensation is too violent.

Maybe it is possible to come up with a different compensation,² which restores the spacetime symmetry, but also keeps this convergent difference regarding the trace of the stress energy tensor (and therefore automatically also the other stress energy component).

Maybe the unexpected convergence for the difference between the local vac-

¹At least in 4 dimensions.

²Or we might be able to make a smart combination of the compensation we used in this thesis and the case without compensation.

uum and the Bunch-Davies vacuum as seen in $\langle \hat{T}_{ii} \rangle$ for $\xi = 1/8$ and $\chi = -1/24$ helps in finding such a more suitable compensation.³

We hope that the properties of the local vacuum that we established are universal and not only valid in de Sitter space using spatially flat slices. This is something that needs to be verified. Especially when we construct the right compensation to make the local vacuum well-behaved in de Sitter space with spatially flat slicing, there is a risk that the compensation only works in this case and that there is no good way to generalise the compensation to a general spacetime or slicing.

To prevent this tailoring, we need to do comparisons in different spaces or using different slices. A first step could be to test the local vacuum using the hyperbolic coordinates of the de Sitter space (see equation (3.13) and appendix A). This is also a good way to test if the local vacuum is internally consistent.

Another option is to perform a similar comparison as in this thesis for the anti-de Sitter space. There it can be compared to the vacuum state defined in [6].

5.2 Minimal coupling

We have also encountered some interesting questions regarding the Bunch-Davies vacuum at minimal coupling. The numerical simulation of the Minkowski vacuum transitioned to de Sitter space does not match the Bunch-Davies vacuum, but the difference (yellow squares in figure 4.2 or figure 4.5) is hard to interpret. It looks like a numerical error, but it is larger than we would expect the numerical error to be. If it is a numerical error, why does it not show up for conformal coupling? And if it is not a numerical error, what causes the weird behaviour? It might be some oscillating effect, caused by the transition in finite time. But then again, why is it only visible at minimal coupling?

If the difference turns out to be real (so not a numerical error), we might conclude that the Bunch-Davies vacuum is not a good vacuum at minimal coupling, since it is unphysical.⁴

5.3 Cutoff regularisation

Another interesting question arises from the observation that the divergence observed for the dimensional regularisation near $d = 4$ only matches the logarithmic divergence in the cut-off regularisation.

It is especially interesting when we look at the difference between the local vacuum and the Bunch-Davies vacuum for $\langle \hat{T}_{ii} \rangle$ and take $\xi = \sqrt{1/48}$ and $\chi = 0$. In this case⁵ the logarithmic divergence vanishes, while the quadratic divergence remains. This means that, according to the dimensional regularisation we have convergence, while according to the cutoff regularisation we have a divergence.

³Note that $\xi = (3/4) * 1/6$ and $\chi = (-1/4) * 1/6$, so the difference is $1/6$. The factors $3/4$ and $-1/4$ might have something to do with the spatial dimensions versus the time dimension.

⁴If you are a strong defender of the Bunch-Davies vacuum you could in this case even argue that minimal coupling is unphysical, since it does not allow the Bunch-Davies vacuum.

⁵Although this case seems unphysical there is no reason why it should be forbidden.

This means one of the regularisation methods is flawed. Possibly something goes wrong with dimensional regularisation when we do the analytical continuation or because we only look at the limit $d \rightarrow 4$, while there may be poles elsewhere that we should consider. Possibly the cutoff regularisation is flawed and the quadratic divergence is only an artefact of breaking the spacetime symmetry and should be ignored.⁶

In [7] the latter hypothesis is supported. It is argued that the quadratic divergences are unphysical and should simply be subtracted.

In addition, in [8] it is argued that the quadratic divergences occurring during cutoff regularisation can be found using dimensional regularisation by expanding around the pole at $d = 2$. The results in this thesis do not support this. E.g. for $\xi = 0$ we do not have divergent differences when using the dimensional regularisation for $d = 2$, while we do have quadratic divergences when using the cutoff regularisation.

⁶Note that the quadratic divergence is not proportional to the metric.

Bibliography

- [1] N. D. Birrell and P. C. W. Davies. *Quantum Fields in Curved Space*. Cambridge Monographs on Mathematical Physics. Cambridge University Press, 1982.
- [2] C. W. Misner, K. S. Thorne, and J. A. Wheeler. *Gravitation*. W. H. Freeman, San Francisco, 1973.
- [3] V. Mukhanov and S. Winitzki. *Introduction to Quantum Effects in Gravity*. Cambridge University Press, 2007.
- [4] S. M. Carroll. *Spacetime and Geometry*. Cambridge University Press, 7 2019.
- [5] I. S. Gradshteyn, I. M. Ryzhik, D. Zwillinger, and V. Moll. *Table of integrals, series, and products; 8th ed.* Academic Press, Amsterdam, Sep 2014.
- [6] C. Dappiaggi and H. R. C. Ferreira. Hadamard states for a scalar field in anti-de sitter spacetime with arbitrary boundary conditions. *Physical Review D*, 94(12), Dec 2016.
- [7] H. Aoki and S. Iso. Revisiting the naturalness problem: Who is afraid of quadratic divergences? *Physical Review D*, 86(1), Jul 2012.
- [8] L. Bian. Renormalization group equation, the naturalness problem, and the understanding of the higgs mass term. *Physical Review D*, 88(5), Sep 2013.
- [9] C. M. Sommerfield. Quantization on spacetime hyperboloids. *Annals Phys.*, 84:285–302, 1974.

Appendix A

The Local Vacuum in Hyperbolic FRW spaces

We consider the metric given by equation (3.13) where we have relabeled the coordinates:

$$ds^2 = dt^2 - \alpha^2 \sinh^2(t/\alpha) [d\rho^2 + \sinh^2 \rho (d\theta^2 + \sin^2 \theta d\varphi^2)] \quad (\text{A.1})$$

If we only consider the region $t > 0$, we can introduce conformal time by taking

$$\eta = \ln(\tanh(t/2\alpha)) \quad (\text{A.2})$$

This yields

$$ds^2 = \frac{\alpha^2}{\sinh^2(\eta)} [d\eta^2 - d\rho^2 - \sinh^2 \rho (d\theta^2 + \sin^2 \theta d\varphi^2)] \quad (\text{A.3})$$

Note that $\eta < 0$, so the scale factor is given by $a(\eta) = -\alpha / \sinh(\eta)$.

We also introduce another set of coordinates, (η, u^i) , defined by

$$\begin{cases} u^1 = \sinh(\rho) \sin(\theta) \cos(\varphi) \\ u^2 = \sinh(\rho) \sin(\theta) \sin(\varphi) \\ u^3 = \sinh(\rho) \cos(\theta) \end{cases} \quad (\text{A.4})$$

We now consider the Klein-Gordon equation, (3.29):

$$[\square + m^2 + \xi R] \phi = 0 \quad (\text{A.5})$$

When we apply the metric, this gives

$$\left(\partial_\eta \partial_\eta - \frac{2}{\tanh(\eta)} \partial_\eta - \Delta_{(3)} + \frac{m^2 \alpha^2 + 12\xi}{\sinh^2(\eta)} \right) \phi = 0 \quad (\text{A.6})$$

Here $\Delta_{(3)}$ is the three-dimensional Laplacian, given by

$$\Delta_{(3)} \phi = \left[\partial_\rho \partial_\rho + \frac{2}{\tanh \rho} \partial_\rho + \frac{1}{\sinh^2 \rho} \left(\partial_\theta \partial_\theta + \frac{1}{\tan \theta} \partial_\theta \right) + \frac{1}{\sinh^2 \rho \sin^2 \theta} \partial_\varphi \partial_\varphi \right] \phi \quad (\text{A.7})$$

We can rescale the field using

$$\tilde{\phi} = \frac{\alpha}{\sinh(\eta)} \phi \quad (\text{A.8})$$

This gives us

$$\left(\partial_\eta \partial_\eta - \Delta_{(3)} + 1 - \frac{2}{\tanh^2(\eta)} + \frac{m^2 \alpha^2 + 12\xi}{\sinh^2(\eta)} \right) \tilde{\phi} = 0 \quad (\text{A.9})$$

We can now write $\tilde{\phi}(\eta, u^i) = \chi_k(\eta) \nu_{k,N}(u^i)$ and use separation of variables to get

$$\begin{cases} \left(\partial_\eta \partial_\eta + \frac{m^2 \alpha^2 + 12(\xi - \frac{1}{6})}{\sinh^2(\eta)} + k^2 \right) \chi_k(\eta) = 0 \\ (\Delta_{(3)} + 1 + k^2) \nu_{k,N}(u^i) = 0 \end{cases} \quad (\text{A.10})$$

The first equation gives solutions $\chi_k(\eta)$ and $\chi_k^*(\eta)$ which can be explicitly given by hypergeometric functions of $\tanh \eta$.

A complete set of normalised solutions of the second equation is given by [9]:

$$\nu_{k,N}(u) = \frac{1}{\sqrt{2\pi^3}} k (N \cdot u)^{-1+ik} \quad (\text{A.11})$$

Here N^μ depends on a complex number z and is given by

$$N^\mu(z) = (1 + |z|^2; -2 \operatorname{Re}\{z\}; -2 \operatorname{Im}\{z\}; 1 - |z|^2) \quad (\text{A.12})$$

The 4-vector u^μ is given by

$$u^\mu = (\cosh(\rho), u^i) \quad (\text{A.13})$$

Our quantum field operator $\hat{\phi}$ is now given by¹

$$\hat{\phi}(\eta, u^i) = \frac{\sinh \eta}{\alpha} \int_0^\infty dk \int d^2 z \left[\chi_k(\eta) \nu_{k,N}(u^i) \hat{a}_{k,N} + \chi_k^*(\eta) \nu_{k,N}^*(u^i) \hat{a}_{k,N}^\dagger \right] \quad (\text{A.14})$$

Where we used the notation

$$\int d^2 z = \int_{-\infty}^\infty d(\operatorname{Re} z) \int_{-\infty}^\infty d(\operatorname{Im} z) \quad (\text{A.15})$$

To be able to construct the local vacuum at a slice $\eta = \eta_0$, we have to express the Minkowski field operator in similar hyperbolic coordinates.

We start with the usual Minkowski coordinates $(\bar{t}, r, \theta, \varphi)$, with the metric

$$ds^2 = d\bar{t}^2 - dr^2 - r^2 (d\theta^2 + \sin^2(\theta) d\varphi^2) \quad (\text{A.16})$$

¹Assuming χ_k is also properly normalised.

If we consider the region $\bar{t} > r$, we can apply the following coordinate transformation to $(\bar{\eta}, \rho, \theta, \varphi)$:²

$$\begin{cases} \bar{t} = e^{\bar{\eta}} \cosh(\rho)/m \\ r = e^{\bar{\eta}} \sinh(\rho)/m \end{cases} \quad (\text{A.17})$$

This gives

$$ds^2 = \frac{e^{2\bar{\eta}}}{m^2} [d\bar{\eta}^2 - d\rho^2 - \sinh^2(\rho)(d\theta^2 + \sin^2(\theta) d\phi^2)] \quad (\text{A.18})$$

So we have the scale factor $a(\bar{\eta}) = e^{\bar{\eta}}/m$.

We have the Minkowski modes in the usual coordinates:

$$u_{\vec{k}}(\bar{t}, \vec{x}) = \frac{1}{\sqrt{2(2\pi)^3\omega}} e^{-i(\omega\bar{t} - \vec{k}\cdot\vec{x})} \quad \text{with} \quad \omega = \sqrt{m^2 + k^2} \quad (\text{A.19})$$

In [9], these are transformed to the new coordinates:

$$u_{k,N}(\bar{\eta}, u^i) = \int d^3k' u_{\vec{k}'}(\bar{t}, \vec{x}) \langle \vec{k}' | k, N \rangle = -\frac{i}{2} \sqrt{\pi} e^{\frac{k\pi}{2}} m e^{-\bar{\eta}} H_{ik}^{(2)}(e^{\bar{\eta}}) \nu_{k,N}(u^i) \quad (\text{A.20})$$

Here u^i and $\nu_{k,N}(u^i)$ are the same expressions as before and $H_\nu^{(2)}(z)$ is the Hankel function of the second kind.

The Minkowski field operator is now written as

$$\hat{\phi}(\bar{\eta}, u^i) = \int_0^\infty dk \int d^2z \left[u_{k,N}(\bar{\eta}, u^i) \hat{a}_{k,N} + u_{k,N}^*(\bar{\eta}, u^i) \hat{a}_{k,N}^\dagger \right] \quad (\text{A.21})$$

We can now construct the local vacuum. We take the slice $\eta = \eta_0$ in de Sitter space and we map this to a slice in Minkowski space with $\bar{\eta} = \bar{\eta}_0$ such that

$$a(\eta_0) = a(\bar{\eta}_0) \quad (\text{A.22})$$

This gives

$$\bar{\eta}_0 = \ln(-m\alpha / \sinh \eta_0) \quad (\text{A.23})$$

Matching the field operators at both slices gives

$$\chi_k(\eta_0) = \frac{i}{2} \sqrt{\pi} e^{\frac{k\pi}{2}} H_{ik}^{(2)}(ma_0) \quad (\text{A.24})$$

Here $a_0 = -\alpha / \sinh(\eta_0)$ is the scale factor at $\eta = \eta_0$.

Matching the momentum operators is a bit more complicated. It gives

$$\partial_\eta \left(\frac{\sinh \eta}{\alpha} \chi_k(\eta) \right) \Big|_{\eta=\eta_0} = \partial_{\bar{\eta}} \left(-\frac{i}{2} \sqrt{\pi} e^{\frac{k\pi}{2}} m e^{-\bar{\eta}} H_{ik}^{(2)}(e^{\bar{\eta}}) \right) \Big|_{\bar{\eta}=\bar{\eta}_0} \quad (\text{A.25})$$

This yields, using equation (A.24)

$$\dot{\chi}_k(\eta_0) = \frac{i}{2} \sqrt{\pi} e^{\frac{k\pi}{2}} \left(\frac{2}{e^{-2\eta_0} - 1} H_{ik}^{(2)}(ma_0) + ma_0 H_{ik}'^{(2)}(ma_0) \right) \quad (\text{A.26})$$

Together with equation (A.24) this fixes the initial conditions of χ_k and this indirectly defines the local vacuum.

²The mass m is used to set a length scale. We could also have chosen another length scale.

Appendix B

Results for Cutoff Regularisation

In this appendix we calculate the cutoff regulated expectation values of the stress energy tensor for the Bunch-Davies vacuum and for the local vacuum.

Bunch-Davies vacuum

Recall the mode expansion, (1.27)

$$\hat{\phi} = \int d^3k \left(u_{\vec{k}}(\eta, \vec{x}) \hat{a}_{\vec{k}} + u_{\vec{k}}^*(\eta, \vec{x}) \hat{a}_{\vec{k}}^\dagger \right) \quad (\text{B.1})$$

The modes are given by equation (3.19):

$$u_{\vec{k}} = v_k(\eta) e^{i\vec{k}\cdot\vec{x}} = \frac{1}{\pi\alpha} \sqrt{\frac{(-\eta)^3}{32}} H_\nu^{(1)}(-k\eta) e^{i\vec{k}\cdot\vec{x}} \quad (\text{B.2})$$

Here $\nu = \sqrt{9/4 - m^2\alpha^2 - 12\xi}$. The function $H_\nu^{(1)}(z)$ is the Hankel function of the first kind. For real ν and z its complex conjugate is given by

$$\left(H_\nu^{(1)}(z) \right)^* = H_\nu^{(2)}(z) \quad (\text{B.3})$$

Here the function $H_\nu^{(2)}(z)$ is the Hankel function of the second kind.

We can calculate:

$$\dot{v}_k(\eta) = \frac{-3}{2\pi\alpha} \sqrt{\frac{(-\eta)}{32}} H_\nu^{(1)}(-k\eta) - \frac{k}{\pi\alpha} \sqrt{\frac{(-\eta)^3}{32}} H_\nu'^{(1)}(-k\eta) \quad (\text{B.4})$$

Here we used the notation $H_\nu'^{(1,2)}(z) = \frac{d}{dz} H_\nu^{(1,2)}(z)$.

This gives

$$\langle \hat{\phi}^2 \rangle_{BD} = \int d^3k (v_k v_k^*) \quad (\text{B.5})$$

$$= -\frac{\eta^3}{8\pi\alpha^2} \int_0^{k_{\max}} dk k^2 H_\nu^{(1)}(-k\eta) H_\nu^{(2)}(-k\eta) \quad (\text{B.6})$$

$$= \frac{1}{8\pi\alpha^2} \int_0^{z_{\max}} dz z^2 H_\nu^{(1)}(z) H_\nu^{(2)}(z) \quad (\text{B.7})$$

Here we have taken $z = -\eta k$. For low z , $H_\nu^{(1,2)}(z)$ behaves as $z^{-\nu}$, [5] so for $\nu < 3/2$ we have no IR-divergence and only the UV-divergence remains.

Since we are only interested in the divergent terms, we can introduce an arbitrarily high lower bound z_0 to our integral:

$$\langle \hat{\phi}^2 \rangle_{BD} = \frac{1}{8\pi\alpha^2} \int_{z_0}^{z_{\max}} dz z^2 H_\nu^{(1)}(z) H_\nu^{(2)}(z) + \text{regular terms} \quad (\text{B.8})$$

Since z_0 can be arbitrarily high, we can substitute the Hankel functions by their asymptotics given by [5]:

$$\begin{aligned} H_\nu^{(1)}(z) &= \sqrt{\frac{2}{\pi z}} e^{i(z-\pi\nu/2-\pi/4)} \left[1 - \frac{\Gamma(\nu+3/2)}{2iz\Gamma(\nu-1/2)} - \frac{\Gamma(\nu+5/2)}{8z^2\Gamma(\nu-3/2)} \right. \\ &\quad \left. + \frac{\Gamma(\nu+7/2)}{48iz^3\Gamma(\nu-5/2)} + \frac{\Gamma(\nu+9/2)}{384z^4\Gamma(\nu-7/2)} + \mathcal{O}(z^{-5}) \right] \\ &= \sqrt{\frac{2}{\pi z}} e^{i(z-\pi\nu/2-\pi/4)} \left[1 - \frac{(\nu^2-1/4)}{2iz} - \frac{(\nu^2-1/4)(\nu^2-9/4)}{8z^2} \right. \\ &\quad \left. + \frac{(\nu^2-1/4)(\nu^2-9/4)(\nu^2-25/4)}{48iz^3} \right. \\ &\quad \left. + \frac{(\nu^2-1/4)(\nu^2-9/4)(\nu^2-25/4)(\nu^2-49/4)}{384z^4} + \mathcal{O}(z^{-5}) \right] \end{aligned} \quad (\text{B.9})$$

$$\begin{aligned} H_\nu^{(2)}(z) &= \sqrt{\frac{2}{\pi z}} e^{-i(z-\pi\nu/2-\pi/4)} \left[1 + \frac{\Gamma(\nu+3/2)}{2iz\Gamma(\nu-1/2)} - \frac{\Gamma(\nu+5/2)}{8z^2\Gamma(\nu-3/2)} \right. \\ &\quad \left. - \frac{\Gamma(\nu+7/2)}{48iz^3\Gamma(\nu-5/2)} + \frac{\Gamma(\nu+9/2)}{384z^4\Gamma(\nu-7/2)} + \mathcal{O}(z^{-5}) \right] \\ &= \sqrt{\frac{2}{\pi z}} e^{-i(z-\pi\nu/2-\pi/4)} \left[1 + \frac{(\nu^2-1/4)}{2iz} - \frac{(\nu^2-1/4)(\nu^2-9/4)}{8z^2} \right. \\ &\quad \left. - \frac{(\nu^2-1/4)(\nu^2-9/4)(\nu^2-25/4)}{48iz^3} \right. \\ &\quad \left. + \frac{(\nu^2-1/4)(\nu^2-9/4)(\nu^2-25/4)(\nu^2-49/4)}{384z^4} + \mathcal{O}(z^{-5}) \right] \end{aligned} \quad (\text{B.10})$$

We also have [5]

$$H'_\nu{}^{(1,2)}(z) = \frac{1}{2} \left(H_{\nu-1}^{(1,2)}(z) - H_{\nu+1}^{(1,2)}(z) \right) \quad (\text{B.11})$$

This gives us

$$\begin{aligned} H'_\nu{}^{(1)}(z) = & \sqrt{\frac{2}{\pi z}} i e^{i(z-\pi\nu/2-\pi/4)} \left[1 - \frac{(\nu^2 + 3/4)}{2iz} - \frac{(\nu^2 - 1/4)(\nu^2 + 15/4)}{8z^2} \right. \\ & + \frac{(\nu^2 - 1/4)(\nu^2 - 9/4)(\nu^2 + 35/4)}{48iz^3} \\ & \left. + \frac{(\nu^2 - 1/4)(\nu^2 - 9/4)(\nu^2 - 25/4)(\nu^2 + 63/4)}{384z^4} + \mathcal{O}(z^{-5}) \right] \end{aligned} \quad (\text{B.12})$$

$$\begin{aligned} H'_\nu{}^{(2)}(z) = & -\sqrt{\frac{2}{\pi z}} i e^{-i(z-\pi\nu/2-\pi/4)} \left[1 + \frac{(\nu^2 + 3/4)}{2iz} - \frac{(\nu^2 - 1/4)(\nu^2 + 15/4)}{8z^2} \right. \\ & - \frac{(\nu^2 - 1/4)(\nu^2 - 9/4)(\nu^2 + 35/4)}{48iz^3} \\ & \left. + \frac{(\nu^2 - 1/4)(\nu^2 - 9/4)(\nu^2 - 25/4)(\nu^2 + 63/4)}{384z^4} + \mathcal{O}(z^{-5}) \right] \end{aligned} \quad (\text{B.13})$$

We get the following useful combinations of asymptotics:

$$I_1 = H_\nu^{(1)}(z)H_\nu^{(2)}(z) = \frac{2}{\pi z} \left(1 + \frac{\nu^2 - 1/4}{2z^2} + \frac{3(\nu^2 - 1/4)(\nu^2 - 9/4)}{8z^4} + \mathcal{O}(z^{-5}) \right) \quad (\text{B.14})$$

$$I_2 = H'_\nu{}^{(1)}(z)H_\nu^{(2)}(z) + H_\nu^{(1)}(z)H'_\nu{}^{(2)}(z) = \frac{2}{\pi z^2} \left(-1 - \frac{3(\nu^2 - 1/4)}{2z^2} + \mathcal{O}(z^{-3}) \right) \quad (\text{B.15})$$

$$I_3 = H'_\nu{}^{(1)}(z)H'_\nu{}^{(2)}(z) = \frac{2}{\pi z} \left(1 - \frac{\nu^2 - 3/4}{2z^2} - \frac{(\nu^2 - 1/4)(\nu^2 - 45/4)}{8z^4} + \mathcal{O}(z^{-5}) \right) \quad (\text{B.16})$$

Hence

$$\begin{aligned} \langle \hat{\phi}^2 \rangle_{BD} &= \frac{1}{8\pi\alpha^2} \int_{z_0}^{z_{\max}} dz z^2 \left[\frac{2}{\pi z} \left(1 + \frac{\nu^2 - 1/4}{2z^2} \right) \right] + \text{regular terms} \\ &= \frac{1}{4\pi^2\alpha^2} \int_{z_0}^{z_{\max}} dz \left[z + \frac{\nu^2 - 1/4}{2z} \right] + \text{regular terms} \\ &= \frac{1}{4\pi^2\alpha^2} \int_{z_0}^{z_{\max}} dz \left[z - \frac{m^2\alpha^2 + 12(\xi - 1/6)}{2z} \right] + \text{regular terms} \end{aligned} \quad (\text{B.17})$$

Similarly, we get

$$\begin{aligned}
 \langle \partial_0 \hat{\phi} \partial_0 \hat{\phi} \rangle_{BD} &= -\frac{\eta^3}{8\pi\alpha^2} \int_0^{k_{\max}} dk \left[\frac{9k^2}{4\eta^2} I_1 - \frac{3k^3}{2\eta} I_2 + k^4 I_3 \right] \\
 &= \frac{1}{8\pi\alpha^2\eta^2} \int_0^{z_{\max}} dz \left[\frac{9z^2}{4} I_1 + \frac{3z^3}{2} I_2 + z^4 I_3 \right] \\
 &= \frac{1}{4\pi^2\alpha^2\eta^2} \int_{z_0}^{z_{\max}} dz \left[z^3 - z \frac{\nu^2 - 9/4}{2} \right. \\
 &\quad \left. - \frac{(\nu^2 - 1/4)(\nu^2 - 9/4)}{8z} \right] + \text{regular terms} \\
 &= \frac{1}{4\pi^2\alpha^2\eta^2} \int_{z_0}^{z_{\max}} dz \left[z^3 + z \frac{m^2\alpha^2 + 12\xi}{2} \right. \\
 &\quad \left. - \frac{(m^2\alpha^2 + 12(\xi - 1/6))(m^2\alpha^2 + 12\xi)}{8z} \right] + \text{reg.}
 \end{aligned} \tag{B.18}$$

$$\begin{aligned}
 \langle \partial_i \hat{\phi} \partial_i \hat{\phi} \rangle_{BD} &= -\frac{\eta^3}{24\pi\alpha^2} \int_0^{k_{\max}} dk k^4 I_1 \\
 &= \frac{1}{24\pi\alpha^2\eta^2} \int_0^{z_{\max}} dz z^4 I_1 \\
 &= \frac{1}{12\pi^2\alpha^2\eta^2} \int_{z_0}^{z_{\max}} dz \left[z^3 + z \frac{\nu^2 - 1/4}{2} \right. \\
 &\quad \left. + \frac{3(\nu^2 - 1/4)(\nu^2 - 9/4)}{8z} \right] + \text{regular terms} \\
 &= \frac{1}{12\pi^2\alpha^2\eta^2} \int_{z_0}^{z_{\max}} dz \left[z^3 - z \frac{m^2\alpha^2 + 12(\xi - 1/6)}{2} \right. \\
 &\quad \left. + \frac{3(m^2\alpha^2 + 12(\xi - 1/6))(m^2\alpha^2 + 12\xi)}{8z} \right] + \text{reg.}
 \end{aligned} \tag{B.19}$$

$$\begin{aligned}
 \text{Re} \left\{ \langle (\partial_i \hat{\phi}) \hat{\phi} \rangle_{BD} \right\} &= \frac{1}{12\pi^2\alpha^2\eta^2} \int_{z_0}^{z_{\max}} dz \left[-z^3 + z \frac{m^2\alpha^2 + 12(\xi - 1/6)}{2} \right. \\
 &\quad \left. - \frac{3(m^2\alpha^2 + 12(\xi - 1/6))(m^2\alpha^2 + 12\xi)}{8z} \right] + \text{reg.}
 \end{aligned} \tag{B.20}$$

$$\begin{aligned}
 \text{Re} \left\{ \langle (\partial_0 \hat{\phi}) \hat{\phi} \rangle_{BD} \right\} &= -\frac{\eta^3}{8\pi\alpha^2} \int_0^{k_{\max}} dk \left[\frac{3k^2}{2\eta} I_1 - \frac{k^3}{2} I_2 \right] \\
 &= \frac{1}{8\pi\alpha^2\eta} \int_0^{z_{\max}} dz \left[\frac{3z^2}{2} I_1 + \frac{z^3}{2} I_2 \right] \\
 &= \frac{1}{4\pi^2\alpha^2\eta^2} \int_{z_0}^{z_{\max}} dz \eta z + \text{regular terms}
 \end{aligned} \tag{B.21}$$

Note that, where needed, we have taken the real part to take the Weyl ordering of the operators.

We can now calculate the expectation values of the stress energy tensor, given by equation (3.30):

$$\begin{aligned}
 T_{\mu\nu} &= (1 - 2\xi)\phi_{;\mu}\phi_{;\nu} + \left(2\xi - \frac{1}{2}\right)g_{\mu\nu}g^{\alpha\beta}\phi_{;\alpha}\phi_{;\beta} - 2\xi\phi_{;\mu\nu}\phi \\
 &\quad + \frac{1}{2}\xi g_{\mu\nu}\phi\Box\phi - \xi\left[R_{\mu\nu} - \frac{1}{2}Rg_{\mu\nu} + \frac{3}{2}\xi Rg_{\mu\nu}\right]\phi^2 \\
 &\quad + \left(\frac{1}{2} - \frac{3}{2}\xi\right)g_{\mu\nu}m^2\phi^2
 \end{aligned} \tag{B.22}$$

This gives

$$\begin{aligned}
 T_{00} &= (1 - 2\xi)\phi_{;0}\phi_{;0} + (2\xi - \frac{1}{2})(\phi_{;0}\phi_{;0} - 3\phi_{;i}\phi_{;i}) - 2\xi\phi_{;00}\phi \\
 &\quad + \frac{1}{2}\xi a_0^2\phi\Box\phi - \xi\left[Ra_0^2/4 - \frac{1}{2}Ra_0^2 + \frac{3}{2}\xi Ra_0^2\right]\phi^2 \\
 &\quad + \left(\frac{1}{2} - \frac{3}{2}\xi\right)m^2a_0^2\phi^2
 \end{aligned} \tag{B.23}$$

We can use

$$\phi_{;00} = a_0^2\Box\phi + 3\phi_{;ii} \tag{B.24}$$

$$\Box\phi = -(m^2 + \xi R)\phi \tag{B.25}$$

$$\phi_{;ii} = \partial_i\partial_i\phi + \frac{1}{\eta}\partial_0\phi \tag{B.26}$$

This gives us

$$\begin{aligned}
 T_{00} &= \frac{1}{2}\partial_0\phi\partial_0\phi - (6\xi - 3/2)\partial_i\phi\partial_i\phi - 6\xi(\partial_i\partial_i\phi)\phi \\
 &\quad - \frac{6\xi}{\eta}(\partial_0\phi)\phi + \left[\frac{1}{2}a_0^2m^2 + \frac{1}{4}a_0^2\xi R\right]\phi^2
 \end{aligned} \tag{B.27}$$

Using our previous expressions we can now calculate

$$\begin{aligned}
 \langle \hat{T}_{00} \rangle_{BD} &= \frac{1}{4\pi^2\alpha^2\eta^2} \int_{z_0}^{z_{\max}} dz \left[z^3 + z \frac{m^2\alpha^2 - 6(\xi - 1/6)}{2} \right. \\
 &\quad \left. - \frac{m^2\alpha^2(m^2\alpha^2 + 12(\xi - 1/6))}{8z} \right] + \text{reg.}
 \end{aligned} \tag{B.28}$$

Similarly we get

$$\begin{aligned}
 T_{ii} &= (1 - 2\xi)\phi_{;i}\phi_{;i} - (2\xi - \frac{1}{2})(\phi_{;0}\phi_{;0} - 3\phi_{;i}\phi_{;i}) - 2\xi\phi_{;ii}\phi \\
 &\quad - \frac{1}{2}\xi a_0^2\phi\Box\phi + \xi\left[Ra_0^2/4 - \frac{1}{2}Ra_0^2 + \frac{3}{2}\xi Ra_0^2\right]\phi^2 \\
 &\quad - \left(\frac{1}{2} - \frac{3}{2}\xi\right)m^2a_0^2\phi^2
 \end{aligned} \tag{B.29}$$

We can simplify this to

$$T_{ii} = \left(\frac{1}{2} - 2\xi\right)\partial_0\phi\partial_0\phi + \left(4\xi - \frac{1}{2}\right)\partial_i\phi\partial_i\phi - 2\xi(\partial_i\partial_i\phi)\phi - \frac{2\xi}{\eta}(\partial_0\phi)\phi + \left[\left(2\xi - \frac{1}{2}\right)a_0^2m^2 + a_0^2\xi R(2\xi - 1/4)\right]\phi^2 \quad (\text{B.30})$$

From this we can calculate

$$\langle \hat{T}_{ii} \rangle_{BD} = \frac{1}{4\pi^2\alpha^2\eta^2} \int_{z_0}^{z_{\max}} dz \left[\frac{z^3}{3} + z \frac{-m^2\alpha^2 + 6(\xi - 1/6)}{6} + \frac{m^2\alpha^2(m^2\alpha^2 + 12(\xi - 1/6))}{8z} \right] + \text{reg.} \quad (\text{B.31})$$

Local vacuum

For the local vacuum, we have different modes, given by equations (3.33) and (3.34):

$$u_{\vec{k}}(\eta_0, \vec{x}) = \frac{1}{\sqrt{2(2\pi a_0)^3 \omega}} e^{i\vec{k}\cdot\vec{x}} \quad (\text{B.32})$$

$$\dot{u}_{\vec{k}}(\eta_0, \vec{x}) = -i \sqrt{\frac{\omega}{2(2\pi)^3 a_0}} e^{i\vec{k}\cdot\vec{x}} \quad (\text{B.33})$$

Here $\omega = \sqrt{m^2 + \chi R + k^2/a_0^2}$.

This gives:

$$\begin{aligned} \langle \hat{\phi}^2 \rangle_L &= \int d^3k (u_{\vec{k}} u_{\vec{k}}^*) \\ &= -\frac{\eta^3}{4\pi^2\alpha^2} \int_0^{k_{\max}} dk \frac{k^2}{\sqrt{m^2\alpha^2 + 12\chi + \eta^2 k^2}} \\ &= \frac{1}{4\pi^2\alpha^2} \int_0^{z_{\max}} dz \frac{z^2}{\sqrt{m^2\alpha^2 + 12\chi + z^2}} \end{aligned} \quad (\text{B.34})$$

There is no IR-divergence, so we can again set our lower bound to z_0 and expand for high values of z :

$$\begin{aligned} \langle \hat{\phi}^2 \rangle_L &= \frac{1}{4\pi^2\alpha^2} \int_{z_0}^{z_{\max}} dz \frac{z^2}{\sqrt{m^2\alpha^2 + 12\chi + z^2}} + \text{regular terms} \\ &= \frac{1}{4\pi^2\alpha^2} \int_{z_0}^{z_{\max}} dz \frac{z}{\sqrt{1 + (m^2\alpha^2 + 12\chi)/z^2}} + \text{regular terms} \\ &= \frac{1}{4\pi^2\alpha^2} \int_{z_0}^{z_{\max}} dz \left[z - \frac{m^2\alpha^2 + 12\chi}{2z} \right] + \text{regular terms} \end{aligned} \quad (\text{B.35})$$

Similarly, we get

$$\begin{aligned}
 \langle \partial_0 \hat{\phi} \partial_0 \hat{\phi} \rangle_L &= -\frac{\eta}{4\pi^2 \alpha^2} \int_0^{k_{\max}} dk k^2 \sqrt{m^2 \alpha^2 + 12\chi + \eta^2 k^2} \\
 &= \frac{1}{4\pi^2 \alpha^2 \eta^2} \int_0^{z_{\max}} dz z^3 \sqrt{1 + (m^2 \alpha^2 + 12\chi)/z^2} \\
 &= \frac{1}{4\pi^2 \alpha^2 \eta^2} \int_{z_0}^{z_{\max}} dz \left[z^3 + z \frac{m^2 \alpha^2 + 12\chi}{2} \right. \\
 &\quad \left. - \frac{(m^2 \alpha^2 + 12\chi)^2}{8z} \right] + \text{regular terms}
 \end{aligned} \tag{B.36}$$

$$\begin{aligned}
 \langle \partial_i \hat{\phi} \partial_i \hat{\phi} \rangle_L &= -\frac{\eta^3}{12\pi^2 \alpha^2} \int_0^{k_{\max}} dk \frac{k^4}{\sqrt{m^2 \alpha^2 + 12\chi + \eta^2 k^2}} \\
 &= \frac{1}{12\pi^2 \alpha^2 \eta^2} \int_0^{z_{\max}} dz \frac{z^3}{\sqrt{1 + (m^2 \alpha^2 + 12\chi)/z^2}} \\
 &= \frac{1}{12\pi^2 \alpha^2 \eta^2} \int_{z_0}^{z_{\max}} dz \left[z^3 - z \frac{m^2 \alpha^2 + 12\chi}{2} \right. \\
 &\quad \left. + \frac{3(m^2 \alpha^2 + 12\chi)^2}{8z} \right] + \text{regular terms}
 \end{aligned} \tag{B.37}$$

$$\begin{aligned}
 \text{Re} \left\{ \langle (\partial_i \hat{\phi} \partial_i \hat{\phi}) \rangle_L \right\} &= \frac{1}{12\pi^2 \alpha^2 \eta^2} \int_{z_0}^{z_{\max}} dz \left[-z^3 + z \frac{m^2 \alpha^2 + 12\chi}{2} \right. \\
 &\quad \left. - \frac{3(m^2 \alpha^2 + 12\chi)^2}{8z} \right] + \text{regular terms}
 \end{aligned} \tag{B.38}$$

$$\text{Re} \left\{ \langle (\partial_0 \hat{\phi} \partial_0 \hat{\phi}) \rangle_L \right\} = 0 \tag{B.39}$$

We can again use

$$\begin{aligned}
 T_{00} &= \frac{1}{2} \partial_0 \phi \partial_0 \phi - (6\xi - 3/2) \partial_i \phi \partial_i \phi - 6\xi (\partial_i \partial_i \phi) \phi \\
 &\quad - \frac{6\xi}{\eta} (\partial_0 \phi) \phi + \left[\frac{1}{2} a_0^2 m^2 + \frac{1}{4} a_0^2 \xi R \right] \phi^2
 \end{aligned} \tag{B.40}$$

to obtain

$$\begin{aligned}
 \langle \hat{T}_{00} \rangle_L &= \frac{1}{4\pi^2 \alpha^2 \eta^2} \int_{z_0}^{z_{\max}} dz \left[z^3 + z \frac{m^2 \alpha^2 + 6\xi}{2} - \right. \\
 &\quad \left. \frac{(m^2 \alpha^2 + 12\chi)(m^2 \alpha^2 + 12(\xi - \chi))}{8z} \right] + \text{reg.}
 \end{aligned} \tag{B.41}$$

Similarly,

$$\begin{aligned}
 T_{ii} = & \left(\frac{1}{2} - 2\xi\right)\partial_0\phi\partial_0\phi + \left(4\xi - \frac{1}{2}\right)\partial_i\phi\partial_i\phi - 2\xi(\partial_i\partial_i\phi)\phi \\
 & - \frac{2\xi}{\eta}(\partial_0\phi)\phi + \left[\left(2\xi - \frac{1}{2}\right)a_0^2m^2 + a_0^2\xi R(2\xi - 1/4)\right]\phi^2
 \end{aligned} \tag{B.42}$$

gives rise to

$$\begin{aligned}
 \langle \hat{T}_{ii} \rangle_L = & \frac{1}{4\pi^2\alpha^2\eta^2} \int_{z_0}^{z_{\max}} dz \left[\frac{z^3}{3} + z \frac{-m^2\alpha^2 + 24\xi(6\xi - 6\chi - 3/4) + 24\chi}{6} \right. \\
 & \left. + \frac{(m^2\alpha^2 + 12\chi)(m^2\alpha^2 - 12(8\xi - 1)(\xi - \chi))}{8z} \right] + \text{reg.}
 \end{aligned} \tag{B.43}$$

Appendix C

Results for Dimensional Regularisation

In this appendix we calculate the dimensional regulated expectation values of the stress energy tensor for the Bunch-Davies vacuum and for the local vacuum.

Bunch-Davies vacuum

The Bunch-Davies vacuum is symmetric, so we can use

$$T_{\mu\nu} = \frac{T g_{\mu\nu}}{d} \quad (\text{C.1})$$

where T is the trace of the stress energy tensor.

We can use that

$$T = m^2 \phi^2 + (d-1) \left(\xi - \frac{d-2}{4(d-1)} \right) \square(\phi^2) \quad (\text{C.2})$$

Furthermore, according to [1] we have

$$\langle \hat{\phi}^2(x) \rangle_{BD} = \frac{\alpha^2}{(4\pi\alpha^2)^{d/2}} \frac{\Gamma(\nu(d) - \frac{1}{2} + d/2) \Gamma(-\nu(d) - \frac{1}{2} + d/2)}{\Gamma(\nu(d) + \frac{1}{2}) \Gamma(-\nu(d) + \frac{1}{2})} \Gamma(1 - d/2) \quad (\text{C.3})$$

Here $\nu(d) = \sqrt{(d-1)^2/4 - m^2\alpha^2 - \xi d(d-1)}$. Note that this expression is independent of x , so $\langle \square(\phi^2) \rangle_{BD}$ vanishes.

This gives:

$$\langle \hat{T}_{\mu\nu} \rangle_{BD} = \frac{m^2\alpha^2}{d(4\pi\alpha^2)^{d/2}} g_{\mu\nu} \frac{\Gamma(\nu(d) - \frac{1}{2} + d/2) \Gamma(-\nu(d) - \frac{1}{2} + d/2)}{\Gamma(\nu(d) + \frac{1}{2}) \Gamma(-\nu(d) + \frac{1}{2})} \Gamma(1 - d/2) \quad (\text{C.4})$$

When we consider the limit $\epsilon = 4 - d \rightarrow 0$, we get

$$\begin{aligned}
\langle \hat{T}_{\mu\nu} \rangle_{BD} &= \frac{m^2}{64\pi^2\alpha^2} g_{\mu\nu} \frac{\Gamma(\nu(4) + 3/2)\Gamma(-\nu(4) + 3/2)}{\Gamma(\nu(4) + \frac{1}{2})\Gamma(-\nu(4) + \frac{1}{2})} (-2/\epsilon + \mathcal{O}(\epsilon^0)) \\
&= -\frac{m^2(1/4 - [\nu(4)]^2)}{32\pi^2\alpha^2} g_{\mu\nu} (1/\epsilon + \mathcal{O}(\epsilon^0)) \\
&= -\frac{m^2(-2 + m^2\alpha^2 + 12\xi)}{32\pi^2\alpha^2} g_{\mu\nu} (1/\epsilon + \mathcal{O}(\epsilon^0)) \\
&= -\frac{m^4\alpha^4 + 12m^2\alpha^2(\xi - 1/6)}{32\pi^2\alpha^4} g_{\mu\nu} (1/\epsilon + \mathcal{O}(\epsilon^0))
\end{aligned} \tag{C.5}$$

Local vacuum

For the local vacuum, we recall the mode expansion, (1.27)

$$\hat{\phi} = \int d^{d-1}k \left(u_{\vec{k}}(\eta, \vec{x}) \hat{a}_{\vec{k}} + u_{\vec{k}}^*(\eta, \vec{x}) \hat{a}_{\vec{k}}^\dagger \right) \tag{C.6}$$

The modes are given given by equations (3.33) and (3.34):

$$u_{\vec{k}}(\eta_0, \vec{x}) = \frac{1}{\sqrt{2(2\pi a_0)^{d-1} \omega}} e^{i\vec{k}\cdot\vec{x}} \tag{C.7}$$

$$\dot{u}_{\vec{k}}(\eta_0, \vec{x}) = -i \sqrt{\frac{\omega}{2(2\pi)^{d-1} a_0^{d-3}}} e^{i\vec{k}\cdot\vec{x}} \tag{C.8}$$

Here $\omega = \sqrt{m^2 + \chi R + k^2/a_0^2}$.

This gives

$$\begin{aligned}
\langle \hat{\phi}^2 \rangle_L &= \int d^{d-1}k (u_{\vec{k}} u_{\vec{k}}^*) \\
&= \frac{2\pi^{d/2-1/2}}{2(2\pi a_0)^{d-1} \sqrt{m^2 + \chi R} \Gamma(d/2 - 1/2)} \\
&\quad \int_0^\infty dk k^{d-2} \left(1 + \left(\frac{k}{a_0 \sqrt{m^2 + \chi R}} \right)^2 \right)^{-1/2} \\
&= \frac{(m^2 + \chi R)^{d/2-1}}{(4\pi)^{d/2-1/2} \Gamma(d/2 - 1/2)} \int_0^\infty dx x^{d-2} (1 + x^2)^{-1/2}
\end{aligned} \tag{C.9}$$

Here we have taken $x = k/(a_0 \sqrt{m^2 + \chi R})$ and used

$$\int d\Omega_{d-1} = \frac{2\pi^{d/2-1/2}}{\Gamma(d/2 - 1/2)} \tag{C.10}$$

To shorten notations, we write

$$S(p, q) = \int_0^\infty dx x^p (1 + x^2)^q \tag{C.11}$$

This gives

$$\langle \hat{\phi}^2 \rangle_L = \frac{(m^2 + \chi R)^{d/2-1}}{(4\pi)^{d/2-1/2} \Gamma(d/2 - 1/2)} S(d-2, -1/2) \quad (\text{C.12})$$

Similarly, we get

$$\langle \partial_0 \hat{\phi} \partial_0 \hat{\phi} \rangle_L = \int d^{d-1} k (\dot{u}_{\vec{k}} \dot{u}_{\vec{k}}^*) = \frac{a_0^2 (m^2 + \chi R)^{d/2}}{(4\pi)^{d/2-1/2} \Gamma(d/2 - 1/2)} S(d-2, 1/2) \quad (\text{C.13})$$

$$\begin{aligned} \langle \partial_i \hat{\phi} \partial_i \hat{\phi} \rangle_L &= \int d^{d-1} k \left((k^i)^2 u_{\vec{k}} u_{\vec{k}}^* \right) \\ &= \frac{a_0^2 (m^2 + \chi R)^{d/2}}{(4\pi)^{d/2-1/2} (d-1) \Gamma(d/2 - 1/2)} S(d, -1/2) \end{aligned} \quad (\text{C.14})$$

$$\begin{aligned} \langle (\partial_i \partial_i \hat{\phi}) \hat{\phi} \rangle_L &= \int d^{d-1} k \left(-(k^i)^2 u_{\vec{k}} u_{\vec{k}}^* \right) \\ &= -\frac{a_0^2 (m^2 + \chi R)^{d/2}}{(4\pi)^{d/2-1/2} (d-1) \Gamma(d/2 - 1/2)} S(d, -1/2) \end{aligned} \quad (\text{C.15})$$

$$\langle (\partial_0 \hat{\phi}) \hat{\phi} \rangle_L = \int d^{d-1} k (\dot{u}_{\vec{k}} u_{\vec{k}}^*) = -i \frac{a_0 (m^2 + \chi R)^{d/2-1/2}}{(4\pi)^{d/2-1/2} \Gamma(d/2 - 1/2)} S(d-2, 0) \quad (\text{C.16})$$

We can rewrite our integral:

$$\begin{aligned} S(p, q) &= \int_0^\infty dx x^p (1+x^2)^q \\ &= \frac{1}{2} \int_0^\infty dx^2 (x^2)^{p/2-1/2} (1+x^2)^q \\ &= \frac{1}{2} \int_0^1 dz z^{-q-p/2-3/2} (1-z)^{p/2-1/2} \\ &= \frac{\Gamma(-q-p/2-1/2) \Gamma(p/2+1/2)}{2\Gamma(-q)} \end{aligned} \quad (\text{C.17})$$

Here we used $z = 1/(1+x^2)$. Note that the last step strictly only holds if $0 < \text{Re}\{p+1\} < \text{Re}\{-2q\}$, which is not always true in our case. Following the discussion in section 4.3, we still apply this last step in any case, implicitly renormalising a divergence.

This yields

$$\langle \hat{\phi}^2 \rangle_L = \frac{1}{(m^2 + \chi R) a_0^2} \frac{a_0^2 (m^2 + \chi R)^{d/2}}{(4\pi)^{d/2}} \Gamma(1 - d/2) \quad (\text{C.18})$$

$$\langle \partial_0 \hat{\phi} \partial_0 \hat{\phi} \rangle_L = \frac{1}{d} \frac{a_0^2 (m^2 + \chi R)^{d/2}}{(4\pi)^{d/2}} \Gamma(1 - d/2) \quad (\text{C.19})$$

$$\langle \partial_i \hat{\phi} \partial_i \hat{\phi} \rangle_L = -\frac{1}{d} \frac{a_0^2 (m^2 + \chi R)^{d/2}}{(4\pi)^{d/2}} \Gamma(1 - d/2) \quad (\text{C.20})$$

$$\langle (\partial_i \partial_i \hat{\phi}) \hat{\phi} \rangle_L = \frac{1}{d} \frac{a_0^2 (m^2 + \chi R)^{d/2}}{(4\pi)^{d/2}} \Gamma(1 - d/2) \quad (\text{C.21})$$

$$\langle (\partial_0 \hat{\phi}) \hat{\phi} \rangle_L = 0 \quad (\text{C.22})$$

We can now calculate the expectation values of the stress energy tensor, given by equation (3.30):

$$\begin{aligned} T_{\mu\nu} &= (1 - 2\xi) \phi_{;\mu} \phi_{;\nu} + (2\xi - \frac{1}{2}) g_{\mu\nu} g^{\rho\sigma} \phi_{;\rho} \phi_{;\sigma} - 2\xi \phi_{;\mu\nu} \phi \\ &\quad + \frac{2}{d} \xi g_{\mu\nu} \phi \square \phi - \xi \left[R_{\mu\nu} - \frac{1}{2} R g_{\mu\nu} + \frac{2(d-1)}{d} \xi R g_{\mu\nu} \right] \phi^2 \\ &\quad + 2 \left[\frac{1}{4} - (1 - \frac{1}{d}) \xi \right] m^2 g_{\mu\nu} \phi^2 \end{aligned} \quad (\text{C.23})$$

This gives

$$\begin{aligned} T_{00} &= (1 - 2\xi) \phi_{;0} \phi_{;0} + (2\xi - \frac{1}{2}) (\phi_{;0} \phi_{;0} - (d-1) \phi_{;i} \phi_{;i}) - 2\xi \phi_{;00} \phi \\ &\quad + \frac{2}{d} \xi a_0^2 \phi \square \phi - \xi \left[R a_0^2 / d - \frac{1}{2} R a_0^2 + \frac{2(d-1)}{d} \xi R a_0^2 \right] \phi^2 \\ &\quad + 2 \left[\frac{1}{4} - (1 - \frac{1}{d}) \xi \right] m^2 a_0^2 \phi^2 \end{aligned} \quad (\text{C.24})$$

We can use

$$\phi_{;00} = a_0^2 \square \phi + (d-1) \phi_{;ii} \quad (\text{C.25})$$

$$\square \phi = -(m^2 + \xi R) \phi \quad (\text{C.26})$$

$$\phi_{;ii} = \partial_i \partial_i \phi + \frac{1}{\eta} \partial_0 \phi \quad (\text{C.27})$$

This gives us

$$\begin{aligned} T_{00} &= \frac{1}{2} \partial_0 \phi \partial_0 \phi - (d-1) (2\xi - 1/2) \partial_i \phi \partial_i \phi - 2\xi (d-1) (\partial_i \partial_i \phi) \phi \\ &\quad - \frac{2\xi (d-1)}{\eta} (\partial_0 \phi) \phi + \left[\frac{1}{2} a_0^2 m^2 + a_0^2 \xi R (1/2 - 1/d) \right] \phi^2 \end{aligned} \quad (\text{C.28})$$

Using our previous expressions we can now calculate

$$\begin{aligned} \langle \hat{T}_{00} \rangle_L &= \frac{a_0^2 (m^2 + \chi R)^{d/2}}{(4\pi)^{d/2}} \Gamma(1 - d/2) \left[\frac{1}{2d} + (d-1)(2\xi - 1/2)/d - 2\xi(d-1)/d \right. \\ &\quad \left. + \frac{m^2}{m^2 + \chi R} \left(\frac{1}{2} + \xi R(1/2 - 1/d)/m^2 \right) \right] \end{aligned} \quad (\text{C.29})$$

In the limit $\epsilon = d - 4 \rightarrow 0$, this gives

$$\begin{aligned} \langle \hat{T}_{00} \rangle_L &= -\frac{a_0^2 (m^2 + \chi R)}{8\pi^2} (1/\epsilon + \mathcal{O}(\epsilon^0)) \left[-\frac{1}{4} (m^2 + \chi R) + m^2 \left(\frac{1}{2} + \frac{\xi R}{4m^2} \right) \right] \\ &= -\frac{(m^2 + \chi R)(m^2 + (\xi - \chi)R)}{32\pi^2} g_{00} (1/\epsilon + \mathcal{O}(\epsilon^0)) \end{aligned} \quad (\text{C.30})$$

Similarly we can look at T_{ii} :

$$\begin{aligned} T_{ii} &= (1 - 2\xi)\phi_{;i}\phi_{;i} - (2\xi - \frac{1}{2})(\phi_{;0}\phi_{;0} - (d-1)\phi_{;i}\phi_{;i}) - 2\xi\phi_{;ii}\phi \\ &\quad - \frac{2}{d}\xi a_0^2 \phi \square \phi + \xi \left[Ra_0^2/d - \frac{1}{2}Ra_0^2 + \frac{2(d-1)}{d}\xi Ra_0^2 \right] \phi^2 \\ &\quad - 2 \left[\frac{1}{4} - (1 - \frac{1}{d})\xi \right] m^2 a_0^2 \phi^2 \end{aligned} \quad (\text{C.31})$$

We can simplify this to

$$\begin{aligned} T_{ii} &= \left(\frac{1}{2} - 2\xi \right) \partial_0 \phi \partial_0 \phi + (2\xi(d-2) - \frac{1}{2}(d-3)) \partial_i \phi \partial_i \phi - 2\xi (\partial_i \partial_i \phi) \phi \\ &\quad - \frac{2\xi}{\eta} (\partial_0 \phi) \phi + \left[(2\xi - \frac{1}{2}) a_0^2 m^2 + a_0^2 \xi R (2\xi - 1/2 + 1/d) \right] \phi^2 \end{aligned} \quad (\text{C.32})$$

resulting in

$$\begin{aligned} \langle \hat{T}_{ii} \rangle_L &= \frac{a_0^2 (m^2 + \chi R)^{d/2}}{(4\pi)^{d/2}} \Gamma(1 - d/2) \left[\frac{\frac{1}{2} - 2\xi}{d} - \frac{2\xi(d-2) - \frac{1}{2}(d-3)}{d} - 2\xi/d \right. \\ &\quad \left. + \frac{m^2}{m^2 + \chi R} \left((2\xi - \frac{1}{2}) + \xi R(2\xi - 1/2 + 1/d)/m^2 \right) \right] \end{aligned} \quad (\text{C.33})$$

In the limit $\epsilon = d - 4 \rightarrow 0$, this gives

$$\begin{aligned} \langle \hat{T}_{ii} \rangle_L &= -\frac{a_0^2 (m^2 + \chi R)}{8\pi^2} (1/\epsilon + \mathcal{O}(\epsilon^0)) \left[\left(\frac{1}{4} - 2\xi \right) (m^2 + \chi R) \right. \\ &\quad \left. + m^2 \left(-\frac{1}{2} + 2\xi + \frac{\xi R}{m^2} (2\xi - 1/4) \right) \right] \\ &= \frac{(m^2 + \chi R)}{32\pi^2} g_{ii} (1/\epsilon + \mathcal{O}(\epsilon^0)) [-m^2 - R(\xi - \chi)(1 - 8\xi)] \\ &= -\frac{(m^2 + \chi R)(m^2 - R(\xi - \chi)(8\xi - 1))}{32\pi^2} g_{ii} (1/\epsilon + \mathcal{O}(\epsilon^0)) \end{aligned} \quad (\text{C.34})$$

